

Electronic Thesis and Dissertation Repository

8-10-2022 10:00 AM

Myeloarchitectonic Maps of Cat Auditory Cortex

Austin Robertson, *The University of Western Ontario*

Supervisor: Butler, Blake E, *The University of Western Ontario*

A thesis submitted in partial fulfillment of the requirements for the Master of Science degree in Neuroscience

© Austin Robertson 2022

Follow this and additional works at: <https://ir.lib.uwo.ca/etd>



Part of the [Animal Experimentation and Research Commons](#), [Cognitive Neuroscience Commons](#), [Neurosurgery Commons](#), [Other Neuroscience and Neurobiology Commons](#), [Speech and Hearing Science Commons](#), and the [Systems Neuroscience Commons](#)

Recommended Citation

Robertson, Austin, "Myeloarchitectonic Maps of Cat Auditory Cortex" (2022). *Electronic Thesis and Dissertation Repository*. 8754.
<https://ir.lib.uwo.ca/etd/8754>

This Dissertation/Thesis is brought to you for free and open access by Scholarship@Western. It has been accepted for inclusion in Electronic Thesis and Dissertation Repository by an authorized administrator of Scholarship@Western. For more information, please contact wlsadmin@uwo.ca.

1.1 Abstract

The cerebral cortex contains myriad cortical areas that differ in structure, function, and connectivity. Current methods of delineating cortical structures and their subregions are insufficient for *in vivo* applications, either being highly invasive or requiring a detailed knowledge of a region's tuning properties. To address this, we seek to establish a structural biomarker capable of delineating the cortex that possesses a non-invasive correlate. We explore myelin as a potential candidate by evaluating its efficacy in parcellating the feline auditory cortex through the generation of depthwise myelin density profiles for each of the 13 auditory cortical subregions. Our analyses revealed significant differences between several auditory cortical subregions, as well as significant correlations between both processing complexity and cortical depth with myelin content. By establishing myelin as a useful biomarker for cortical parcellation, we hope to better describe the brain regions and networks that underlie complex human behaviours and reorganized function.

Keywords: Myelin, Auditory Cortex, Cortical Parcellation, Biomarker, SMI-32, Processing Hierarchy

Summary for Lay Audience

The brain comprises a number of distinct regions, each of which makes unique contributions to one or more complex behaviours. For example, the region of the brain responsible for perceiving sounds (i.e., the auditory cortex), has traditionally been thought of as distinct from the region that makes sense of what we see (i.e., the visual cortex). Moreover, within a region like the auditory cortex, there exist subregions that are sensitive to the many different features of sound. For example, core auditory areas are typically involved in identifying that a sound is present in the environment, while higher-order areas are sensitive to features including direction of motion, or a speaker's identity. The ability to identify the location of these distinct regions in the brain is essential to understanding their function, and is especially useful in identifying the source atypical brain activity, and in designing therapies to help affected individuals. Localizing specific areas of the brain often relies on the ability to visualize characteristic patterns of brain activity; however, this limits our ability to accurately locate areas of interest in people who have atypical function (e.g. blindness, deafness, etc.), or to discern between parts of the brain that are activated by the similar stimuli or processes. Thus, the work described here uses a structural property of the brain – patterns of myelin content – to discern between regions of the feline auditory cortex. Myelin is present throughout the brain, and previous research has suggested that small but distinct regions of the brain can be distinguished from one-another based on their total myelin content. We demonstrate that many subregions of the auditory cortex differ with respect to their total myelin content, with core areas containing the most myelin, and higher-order areas containing significantly less. These results suggest there are predictable changes in the myelin content of the auditory cortex between regions, suggesting that myelin may be a useful structural marker for parcellating the auditory brain.

Co-Authorship Statement

All research conducted in this thesis was in collaboration with my supervisor, Dr. Blake Butler. Additionally, methodological training and assistance was provided by Dr. Daniel J Miller, and histological assistance was provided by Adam Hull.

Acknowledgments

First and foremost, I would like to thank my supervisor, Dr. Blake Butler, for his guidance and support. He has been a tremendous mentor and friend throughout these past two years. His ingenuity, creativity, and infectious love for his craft have inspired me and helped me grow as both a scientist and a student throughout my graduate degree. I am honoured to be among the first graduate students to come through his lab and look forward to our continued partnership as I complete my doctoral work under his wing.

I would also like to thank the other members of the Nissl lab who have kept me sane and who have helped me throughout my time here. I would especially like to thank Katelyn Kittel for her tireless work in keeping our animals happy and healthy and for being such a positive force in every lab meeting, colony visit, or random encounter in any hallway of the SSC. Furthermore, a special thanks to Adam Hull, who has consistently gone above and beyond in all things asked of him and without whom the histology work would have been infinitely more difficult.

Thank you to my advisors, Dr. Brian Allman, Dr. Corey Baron, Dr. Paul Gribble, and Dr. Udunna Anozodo for their expertise and their coaching. I always left our committee meetings with a positive outlook on my project, and new ideas to better collect and represent my data. Your feedback and guidance were invaluable and without them, this work would not exist.

Lastly, my personal thank yous. First, my parents, who allowed me to move home so I could afford to pursue my graduate degree, and who have been my greatest supporters for the past 24 years. My little brothers, who inspire me and for whom I make every effort to be an inspiration. My basketball players, who bring me joy and remind me there is more to life than school. Finally, my partner Alex - for everything, always.

Table of Contents

Abstract.....	ii
Summary for Lay Audience.....	iii
Co-Authorship Statement.....	iv
Acknowledgments.....	v
Table of Contents.....	vi
List of Figures.....	viii
List of Tables.....	viii
List of Appendices.....	ix
Chapter 1.....	1
1 Introduction.....	1
1.1 A brief history of cortical segmentation.....	1
1.2 Myelin as a Biomarker.....	5
1.3 Quantifying patterns of myelination.....	8
1.3.1 Histological Quantification.....	9
1.3.2 MRI-based estimates of myelination.....	11
1.4 The Auditory Cortical Processing Hierarchy.....	13
1.5 Current Study.....	16
Chapter 2.....	17
2 Methodology.....	17
2.1 Tissue Preparation.....	17
2.2 SMI-32 Immunohistochemistry.....	18
2.3 Myelin Visualization.....	18
2.4 Myelin Quantification.....	19
2.5 Statistical Analysis.....	21

Chapter 3.....	23
3 Results.....	23
3.1 Myelin Differences Across Anatomical Borders.....	23
3.2 Stereological Quantification of Myelin: Accordance with the Processing Hierarchy, Effect of Depth, and Quantitative Comparisons Between Sub-Regions	27
4 Discussion.....	34
4.1 Patterns of Myelin Length Density in Auditory Cortex.....	35
4.2 Hierarchical Distribution of Myelin in Auditory Cortex.....	35
4.3 Basis for Cortical Delineation Based on Myeloarchitecture.....	39
4.4 Limitations.....	41
4.4.1 Limitations in Sample Size.....	41
4.4.2 Methodological Limitations.....	41
4.5 Future Directions.....	42
4.6 Conclusion.....	43
References.....	44
Appendix A.....	52
Curriculum Vitae.....	53

List of Figures

Figure 1-1 The Cortical Maps of Ferrier in the Primate (left) and Human (right) Brains (Adapted from Morabito, 2013).....	2
Figure 1-2 Localization of human brain functions as described in 1957 based on lesion and brain stimulation studies (Polyak, 1957).	4
Figure 1-3 The Structure of the Myelin Sheath	6
Figure 1-4 The Spaceballs Probe	11
Figure 1-5 The Subregions of the Cat Auditory Cortex and the Processing Hierarchy	15
Figure 2-1 Transfer of ROIs from SMI-32 to Myelin-Stained Sections.....	20
Figure 3-1 Photomicrographs of Auditory Cortical Subregions.....	24
Figure 3-2 Columnar Photomicrographs of Auditory Cortical Subregions.....	26
Figure 3-3: A Visual Representation of the Spaceballs Probe.....	28
Figure 3-4: Normalized Myelin Length Density Across Two Cats	29
Figure 3-5: Myelin Length Density Collapsed Across Depths Within Subregions	31
Figure 3-6: Volume Weighted Myelin Length Density vs. Subregion Level on Processing Hierarchy.....	33
Figure 4-1: Lateral View of Cat Brain With Myelin Length Density Heat Map.....	39

List of Appendices

Appendix A: CE Values..... 53

Chapter 1

2 Introduction

2.1 A brief history of cortical segmentation

For more than 200 years, scientists have sought to understand complex behaviours by ascribing functions to different subregions of the brain. At the outset of the 19th century, Franz Joseph Gall's phrenological doctrine proposed that the cortex could be divided into 27 "organs", each of which corresponded to a particular character trait (these included courage, humour, and religious veneration, among many others). He believed that the size of these "organs" was reflective of their functional strength, and that larger organs would inevitably lead to prominences in the bones of the skull (Simpson, 2005). Thus, he proposed that one could glean an understanding of the personality and intellectual capacity of a person by feeling their skull and noting where these prominences occurred - an idea that had profound influence on the fields of psychiatry, law, education, and neurosurgery (Simpson, 2005). While phrenology has long since been dismissed as pseudoscience, the idea the brain exhibits a high degree of compartmentalization and functional specialization persists in neuroscientific study.

Many early studies that endeavored to ascribe functions to cortical subregions established relationships between behavioural deficits and underlying neural pathology. For example, in 1861, French neurosurgeon Paul Broca examined the brain of the recently deceased "patient Tan", who had notable impairments in the ability to communicate using spoken or written language despite no apparent motor deficits (Broca, 1865). An autopsy revealed a significant lesion in the left frontal cortex, a region Broca concluded was responsible for language production, but had no bearing on language comprehension or other associated cognitive functions (Broca 1865). This finding was subsequently supported by case reports of other aphasic patients who presented with similar lesions. Nearly a decade later, German neurologist Carl Wernicke would go on to describe how focal damage to a region of the left temporal lobe produce a different pattern of aphasia, in which speech understanding and the ability to produce meaningful syntax are severely

impaired while the motoric elements of speech production are unaffected. This demonstration of double dissociation of speech production and reception in the brain served as compelling evidence of functional specialization within the brain. However, still haunted by the specter of phrenology, there remained a large and vocal group of “anti-localizationists” who rejected the idea that the brain was functionally compartmentalized and who remained prominent until the eve of the 20th century.

David Ferrier was a Scottish neurologist who set out to prove that unique functions *could* be ascribed to different brain regions and create detailed functional maps of the cortex. Using stimulation and ablation techniques, Ferrier was able to localize several key structures within the brain with remarkable accuracy given the methodological constraints of the time (Heffner, 1987; Figure 1-1). This included the cerebral motor centres (Millett, 1998), as well as regions of the superior temporal gyrus of the monkey in which ablations consistently led to deafness (auditory cortex; Heffner, 1987). At the International Medical Congress of 1881, Ferrier would debate prominent anti-localizationist Friedrich Leopold Goltz; his demonstrations that monkeys with identical ablations exhibited identical functional deficits limited exclusively to specific cognitive functions, and not others established the consensus opinion in support of functional specialization and proved to be a defining moment in the field of neuroscience (Tyler and Malessa, 2000).

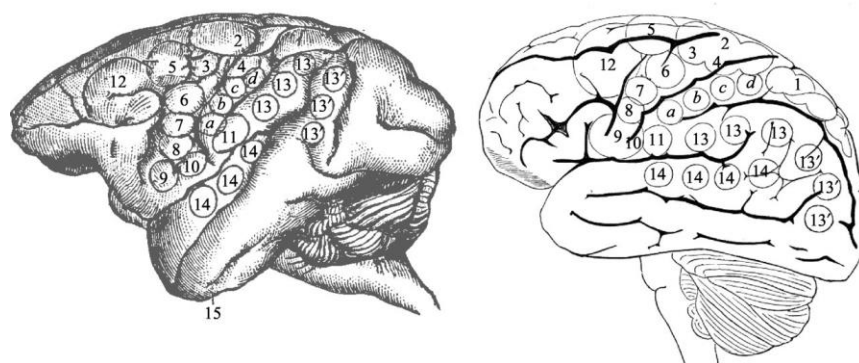


Figure 2-1 Ferrier’s cortical maps of the macaque (left) and human (right) brain (Adapted from Morabito, 2013)

These early efforts to describe the functional specialization of cortical subregions were foundational in our understanding of how the brain is organized. However, their reliance on establishing relationships between behavioural deficits and underlying pathology had several limitations. Firstly, human case studies often included severe damage to the cortex, brought on by either brain injury/trauma or ischemic stroke. As a result, damage was often far-reaching and extended across borders between cortical areas, making it difficult to draw causal inferences between damage to a specific brain region and resulting functional deficits. To remedy this, Korbinian Brodmann, a German neuroscientist, decided to create an atlas of the brain that was based on structural features, with the idea that the functional distinctions between areas likely had some form of anatomical underpinning that could be used to identify them. In 1909, he published his seminal work “Localization in the Cerebral Cortex” in which he divided the brain into 52 distinct areas, based on their cytoarchitecture (Zilles, 2018; Annese, 2009). “Brodmann’s areas” served as a probabilistic atlas of the brain against which functional data could be compared, and within which it could be contextualized. A 2009 article poignantly summarized Brodmann’s enormous influence on the field as follows: “[His] classic neurology text written 100 years ago still provides the core principles for linking the anatomy of the cerebral cortex to its function today” (Annese, 2009).

Guided by Brodmann’s map, Canadian neurosurgeon Wilder Penfield explored the effects of direct electrical stimulation on cortical areas exposed during neurosurgery (Savoy, 2001; Penfield and Jasper, 1954). By stimulating specific brain regions in conscious human subjects, Penfield was able to explore causative structure-to-function relationships in the brain with much greater resolution than had been provided by lesion studies. He was also able to replicate this work across a number of subjects, to assess how well these relationships were preserved across individuals. As a result, by the late 1950s a highly detailed map of cortical function had emerged that is largely consistent with our modern understanding (Polyak, 1957; Figure 1-2).



Figure 2-2 Localization of human brain functions as described in 1957 based on lesion and brain stimulation studies (Adapter from Polyak, 1957).

In the 65 years since this figure was first published, rapid advances in non-invasive functional neuroimaging (e.g., positron emission tomography [PET], functional magnetic resonance imaging [fMRI]) and transcranial manipulation of neural activity (e.g., transcranial magnetic stimulation [TMS], transcranial alternating/direct current stimulation [tACS/tDCS]) have extended upon this framework, providing a great deal more nuance and spatial resolution to cortical maps.

In particular, fMRI has become a widely used tool in both research and clinical settings to map areas of the brain based on activity, often relying on functional localizer scans that are designed to identify those specific brain regions that are involved in a particular behaviour. New fMRI work is published every day (Glover, 2011), largely because fMRI is non-invasive, widely available, has relatively high spatiotemporal resolution, and can demonstrate activity within entire networks of brain regions that are engaged during the performance of tasks or the presence of specific stimuli/stimulus features (Logothetis, 2008). fMRI, in conjunction with other modern brain mapping techniques, has thus

dramatically accelerated our understanding of the neural correlates of a broad range of functions, as well as the diverse connective networks into which these areas assemble. However, several limitations remain. First, in many cases brain regions are identified using functional localizers that identify regions of the brain based on known response characteristics (e.g., the fusiform face area can be localized by determining which region of the brain responds robustly to faces but not to other objects like houses). Thus, functional localizers are of little value when specific response properties of cortical subregions have not yet been well defined. For example, the feline auditory cortex has 13 distinct but highly interconnected areas; however, the tuning properties of these regions are not understood to a level that would allow for the design of 13 unique functional localizers that would limit co-activation among areas. Furthermore, the identification of distinct cortical areas using functional localizers is poorly suited to the study of clinical populations defined by atypical activity in these areas (e.g., D/deaf participants).

Thus, there has been great interest in establishing robust methods for identifying cortical subregions using structural biomarkers for which non-invasive imaging sequences have been developed. A number of potential biomarkers have been identified; however, determining the validity of these measures requires a highly invasive histological approach that lacks applicability for in vivo human applications.

2.2 Myelin as a Biomarker

Myelin is a lipid-based substance that is generated by oligodendrocytes in the central nervous system (CNS) and Schwann cells in the peripheral nervous system, and which ensheaths and insulates the axons of neurons. As the current thesis is focused on the myeloarchitecture of auditory cortex, the remainder of this section will address myelin formation in the CNS. Myelinating oligodendrocytes are derived from oligodendrocyte precursor cells that increase in number drastically throughout prenatal and postnatal stages of development, and which remain active - though less abundant - in the CNS well into adulthood (Mount and Monje, 2017). Functionally, myelin sheaths allow for the rapid propagation of action potentials along axons, increasing transduction speeds to a

level that would otherwise require prohibitively large axonal diameters to achieve (Williamson and Lyons, 2018). Myelin is arranged along axons in internodal segments that are separated by small unmyelinated gaps referred to as nodes of Ranvier, at which many voltage-gated sodium channels are clustered (Figure 1-3). The clustering of sodium channels at these nodes, combined with the decreased membrane capacitance and increased membrane resistance along insulated portions of the axon, allows for the rapid saltatory conduction speeds characteristic of myelinated axons (Purger et al. 2016). From an evolutionary development perspective, myelinated axons are considered essential to achieving the temporal resolution necessary for the higher order cognitive functions that are the hallmarks of complex nervous systems (Sherman and Brophy, 2005). Consequently, myelin development has been shown to correlate with the onset of typical circuit function, and the emergence of complex cognitive processes in children (Scantlebury et al. 2014).

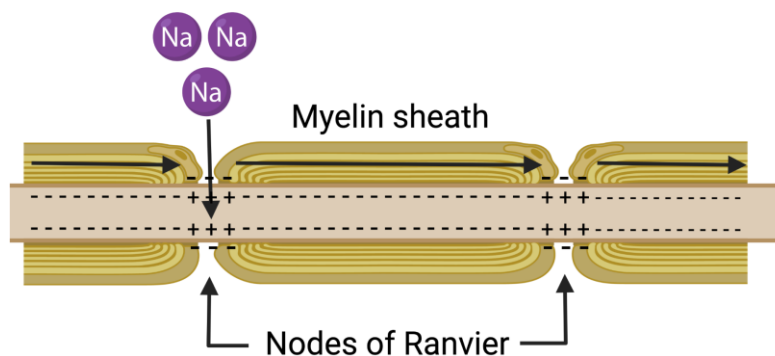


Figure 2-3 The Structure of the Myelin Sheath. Myelinated internodes (yellow) are separated by nodes of Ranvier that are rich in voltage-gated sodium channels. This arrangement facilitates the rapid propagation of the action potentials along the axon.

While the process of myelination occurs predominantly during early childhood, it continues throughout the entirety of the lifespan in a process known as adaptive myelination. Specifically, research suggests that changes in cortical myelination may play a role in experience-dependent functional plasticity following skill learning. For example, learning to juggle (Scholz et al. 2009), and playing a computer game (Hofstetter et al. 2013) have been linked to significant changes in myeloarchitecture within regions of the brain associated with visuomotor skill acquisition and spatial memory, respectively. A number of mechanisms have been proposed to underlie these changes: pre-existing oligodendrocytes may either lengthen or thicken existing myelin sheaths to improve their conductive speed; the nodes of Ranvier may be shortened to increase the concentration of the existing sodium channels; or undifferentiated precursor cells may mature into novel oligodendrocytes that can then myelinate previously unmyelinated segments of axons (Kaller et al. 2017).

This model of myelin plasticity makes sense in the context of cortical adaptation. It is well-established that experience and learning shape functional cortical networks (Zilidou et al. 2018; Kao et al. 2020; Sun et al. 2007; Scholz et al. 2009). This experience-dependent plasticity is reflected at the neuron level by the increased strength of synaptic connections (Litwin-Kumar and Doiron, 2014; Lisman et al. 2018; Shors and Matzel, 1997), which might be expected to place increased demands on these reorganized pathways for efficient conduction of action potentials. Concurrently, then, one might expect to see changes in the underlying myeloarchitecture associated with these networks to reflect these increased demands. That myelin is present and can be quantified regardless of functional status, is closely associated with functional cortical networks that underlie perceptual and cognitive functions, and can reflect subject-specific patterns of experience are good reasons to consider myelination as a biomarker for segmenting the various regions of the brain.

During development, myelination proceeds in a predictable spatiotemporal pattern, with areas dedicated to basic homeostasis becoming myelinated first, and areas dedicated to higher-order complex cognitive functions becoming myelinated last (Brody et al. 1987, Kinney et al. 1988). This gradient of myelin density is exacerbated by the fact that axons

in regions that are myelinated early are also myelinated more completely (Stadelmann et al. 2019). The result is that, within typically developed sensory cortices, primary areas exhibit the highest myelin density, with decreasing myelination observed at each subsequent step along the functional hierarchy (Glasser et al. 2014; Glasser and Van Essen, 2011). This myelin gradient across functional hierarchies likely affects neuroplastic potential, as myelin appears to limit novel synapse formation or rearrangement, and may contribute to the observation that heavily myelinated regions like core sensory cortical areas often exhibit limited neuroplasticity (Glasser, 2014; McGee et al. 2005). In contrast, higher-order regions that are sparsely myelinated exhibit a higher degree of functional and structural plasticity in response to function loss or deficit.

Though there are several structural features that vary across regions of cortex, myelin has emerged as a promising candidate to improve cortical segmentation. Some previous research has established that patterns of myelination reflect the position of cortical regions along the functional hierarchies to which they belong, suggesting that sensory cortices may be delineable based on myelin density. Furthermore, there is evidence that cortical myelination is linked to the pathways underlying changes in the brain's functional connectivity. Therefore, myelin may be useful in creating subject-specific maps that reflect individual experience and learning. Finally, myelin can be measured noninvasively (see Section 1.3 for review); thus, myeloarchitectonic maps could be used effectively in research and clinical applications involving human participants.

2.3 Quantifying patterns of myelination

Myelin is an important part of neuronal axons that provides structural support, and plays a critical role in facilitating rapid electrical transduction, improving the temporal resolution of neural signaling. There are several ways to visualize and quantify myelin density within cortical subregions – both invasive and non-invasive. Here I provide descriptions of several popular histological methods for quantifying myelin, and briefly introduce some of the non-invasive approaches that are used to provide correlated measures.

2.3.1 Histological Quantification

There are many ways to visualize myelinated fibers in the central nervous system. Luxol Fast Blue is a myelin sheath stain that allows for visualization of phospholipids (the main component of myelinated axons; Kluver and Barrera, 1953), and has largely replaced the Weil and Pal-Weigert methods. Unfortunately, while Luxol Fast Blue can help approximate borders between auditory cortical areas (Pistori et al. 2006), it does not allow for the visualization of individual myelinated fibers, which is necessary to quantify the differences between regions using, for example, stereological estimates of fiber length density. Immunocytochemical localization techniques that target myelin basic protein provide good resolution of fibers in sparsely-myelinated areas; however, fibers are poorly resolved in more densely myelinated areas. Thus, myelin basic protein is often unable to provide useful estimates for regions of interest that include cortical layers III through VI (Pistori et al. 2006).

Conversely, the Gallyas approach (Gallyas, 1979) allows individual myelinated fibers to be visualized across all 6 layers of the cortex. The Gallyas protocol uses silver impregnation, which takes advantage of myelin's strong affinity for silver particles following incubation with pyridine and acetic anhydride (note: silver is bound poorly by other tissues in the CNS providing high contrast visualization of myelinated fibers; Gallyas, 1979, Pistori et al. 2006, Joseph et al. 2019). The Gallyas protocol also employs a bleaching step which removes artifactual staining and further improves the contrast between the darkly myelinated axon tracts and the translucent underlying tissue (Pistori et al. 2006, Joseph et al. 2019). The result is a staining protocol that allows for disambiguation of individual axon fibers within each layer of cortex with high resolution and little artifactual staining.

Once myelinated fibers have been stained, the myelin length density of any region of interest can be estimated using stereological techniques. Stereology allows an observer to generate three-dimensional estimates of anatomical features that derive from data acquired by serially analyzing 2-dimensional cross sections of tissue (i.e., annotation of cell features made while scrolling through the z-plane of a mounted tissue sample). Unbiased stereology requires that all sampling is random and systematic and is predicated

on both geometric (Cavalieri's principle) and statistical sampling principles. Cavalieri's principle describes how the volume of a solid can be computed from the volume of cross-sectional slabs comprising that solid, irrespective of their relative arrangement in space. When combined with effective sampling techniques, these principles allow for unbiased estimates that are widely regarded as the gold standard for quantitative histology, and which can accurately quantify cell number, length density, and area/volume of biological structures (West, 2018; MBF Biosciences).

Since myelin is a linear structural feature, an estimate of the total length of myelinated fiber present within a given region of interest is a highly detailed way to quantify how patterns of myelination vary across brain areas. To compute length density estimates, the Spaceballs method (West, 2018) places a series of spatially distributed hemispheric probes in a systematic random fashion across the breadth of a region of interest (systematic in that the probe locations are evenly spaced along the x- and y-axes, but random in that the grid is placed randomly over the ROI). The observer then focuses through the extent of the z-plane and marks any place that a linear feature of interest intersects with the surface of the probe (West, 2018) (Figure 1-5). When a sufficient number of probes have been completed across sections, the total length of myelin present and the myelin length density within each ROI can be mathematically estimated. Additional details regarding the Spaceballs probe and related equations can be found in Section 2.4.

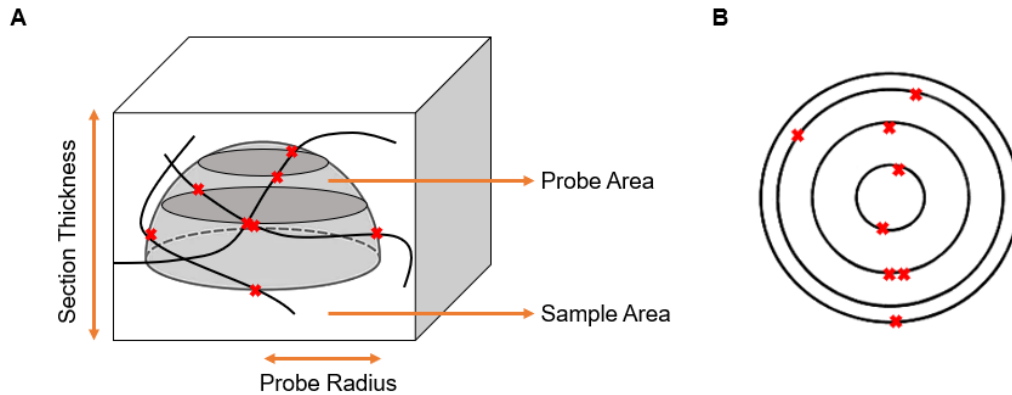


Figure 2-4 The Spaceballs Probe. (A) A hemispheric probe of known volume is virtually embedded into a parcel of tissue. Intersections of linear features of interest (e.g., myelinated fibers) with the areal boundaries of the probe are designated with a marker. Length density is computed from the number of markers in a given region of tissue (See section 2.4). (B) Because we can't impose 3-D shapes in tissue in virtual space, the probe is functionally a stack of concentric circles of varying radii, and markers are placed where in-focus linear features intersect with the perimeter of these concentric circles.

2.3.2 MRI-based estimates of myelination

Magnetic resonance imaging (MRI) is a non-invasive approach that can be used to create detailed three-dimensional anatomical images. MRI uses strong magnets to produce a magnetic field that creates a preferred alignment of the magnetizations of protons found in water molecules that make up living tissues, then passes a radiofrequency pulse through the tissue, exciting the protons before allowing them to realign with the magnetic field (Huettel et al., 2014). This relaxation following the radiofrequency pulse releases energy that is detected by the MRI sensors, which form detailed images based from this information (Huettel et al., 2014). There are two independent relaxation processes: spin-lattice (also called T1 or longitudinal) relaxation is the process of remagnetization in the same direction as the magnetic field; spin-spin (also called T2 or transverse) relaxation

represents the loss of coherence in the transverse direction due to local effects on spin. Importantly, MRI images weighted towards either T1 or T2 relaxation can be used to create anatomical images of tissue that are sensitive to different feature contrasts between structures, and both are important in the non-invasive visualization of myelin.

Myelin is diamagnetic, which influences the strength of the local magnetic field and has an effect on T2 relaxation (Lazari and Lipp, 2021, Moller et al. 2019, Weiskopf et al. 2015). Furthermore, the myelin sheath is rich in macromolecules such as lipids and proteins that can have significant effects on both T1 and T2 relaxation rates (Lazari and Lipp, 2021, MacKay et al. 2009). The fact that densely myelinated areas return high signal intensities in T1-weighted images, and low signal intensity in T2-weighted images has been leveraged to quantify myelination in the central nervous system using T1/T2 ratio images (Glasser and Van Essen, 2011). This approach significantly improves the localization of cortical areas by increasing the contrast between densely and lightly myelinated regions and has been used in conjunction with existing cytoarchitectonic, anatomical, and functional data to produce detailed maps of the cerebral cortex (Glasser and Van Essen, 2011).

Myelin water fraction imaging is another method, and takes advantage of variability in water T2 relaxation times. Water is abundant in the brain, making up for about 70-85% of its total mass (MacKay and Laule, 2016). This water is broadly found in 3 locations - intracellularly, extracellularly, or in the myelin sheath (“myelin water”; MacKay et al. 2016). The T2 relaxation time of intra/extracellular water is far greater than that of myelin water (MacKay and Laule, 2016). Thus, the proportion of the water within a given voxel that is contained within myelin (and by extension the proportion of the voxel that comprises myelin) can be estimated from T2 decay curve by dividing the area under the myelin water T2 curve by the total area of the T2 distribution.

A number of other MRI-based acquisitions can also be used to localize and quantify patterns of myelination. For example, magnetization transfer imaging leverages the phenomenon whereby a proton bound to a macromolecule (e.g. myelin) that is excited by a radiofrequency pulse will transfer a part of its energy to neighbouring unbound protons

(Hagiwara et al. 2018; Henkelman et al. 2001). Because protons in macromolecules are not normally visible using conventional MRI, this indirect method of quantifying their effect on unbound adjacent visible protons serves as a useful proxy measure for their quantification. As a result, magnetization transfer imaging has been shown to be strongly correlated with histological myelin content (Schmierer et al. 2004).

Finally, measures based on the direction of water diffusion within voxels can also be used to estimate myelin content. The structure of the myelin sheath surrounding neurons serves to hinder diffusion across the lipid-rich membrane - constraining the movement of water molecules (which contain the excitable protons measured by MRI) and imposing directionality or anisotropy on them (Lazari et al. 2021). The degree to which the motion of water in the underlying tissue is free/restricted can be measured using specialized diffusion-weighted scans (e.g. diffusion tensor imaging) that are sensitive to the direction and rate of water molecule movement (Aung et al. 2013). Diffusion weighted scans are particularly useful in measuring changes in myelination over time, and are often used in studies pertaining to myelin remodeling including demyelination related to pathology (e.g. multiple sclerosis, sensory loss) and adaptive myelination following learning (Aung et al. 2013, Karns et al. 2017, Kolasa et al. 2019, Scholz et al. 2009).

To summarize, there are a wide variety of methods based in detailed histological assessment and non-invasive neuroimaging that are able to quantify myelin content within specific regions of the brain, and which could be used to segregate unique brain regions based on their myeloarchitecture. Because these approaches are sensitive to anatomical features, this segmentation approach can be undertaken even where the unique functions of cortical subregions are poorly understood (e.g., feline auditory cortex) or where function is atypically developed (e.g., in the D/deaf).

2.4 The Auditory Cortical Processing Hierarchy

A long-established model of hierarchical organization within the *visual* cortex proposes that information passes through the primary visual cortex and is directed along the dorsal

and/or ventral pathways that process cues related to an object's location and identity, respectively (Mishkin et al. 1983). More recently, a similar hierarchical parallel processing framework has been proposed to exist in auditory cortex (Rauschecker and Tian, 2000). In the cat, the 13 regions of auditory cortex are thought to be arranged within parallel functional hierarchies that have been established based on detailed quantifications of cortical and thalamic inputs, synaptic connectivity, and neuronal response properties (Lee and Winer, 2011; Carrasco and Lomber, 2009; Hackett, 2011). Based on their patterns of thalamocortical input (Lee & Winer, 2008a) and studies of their functional properties (e.g., Reale & Imig, 1980; Carrasco & Lomber, 2009) the primary auditory cortex (A1) and anterior auditory field (AAF) in the cat are considered “core” regions that comprise the first tier of the dorsal and ventral processing hierarchies, respectively. While the remainder of the regions comprising the feline auditory cortex are less studied, their positions within the functional hierarchies have been predicted based on their patterns of connectivity (Lee and Winer 2008a; 2008b) In some cases, the proposed relationships between cortical subregions have been supported by observations of function. For example, the posterior auditory field (PAF) and ventral posterior auditory field (VPAF) have been shown to be tonotopically organized (Reale & Imig, 1980) – suggesting they are involved in low-level sound processing. Moreover, deactivation studies have revealed that patterns of activity in PAF are dependent upon A1 activity (Carrasco and Lomber, 2009), and that deactivation of PAF and the dorsal zone of auditory cortex leads to deficits in auditory localization and sound motion discrimination, respectively (Malhotra and Lomber, 2007; Lomber and Malhotra, 2008). Thus, these functional studies support the idea that PAF and DZ are regions that lie downstream of A1 in the dorsal auditory processing stream.

There is a general trend across sensory cortices wherein primary sensory areas (core areas) are heavily myelinated, with decreasing levels of myelination as you progress upwards in the processing hierarchy (Glasser, 2011). Indeed, human neuroimaging studies of cortical myeloarchitecture suggest that across modalities, core sensory areas show greater myelin density than the surrounding tissue (Lutti et al., 2014). While there is still work to be done to validate the model proposed by Lee and Winer (2011; Figure 1-

6), it provides a well-reasoned framework within which to evaluate the relationship between functional hierarchies and myeloarchitecture in auditory cortex.

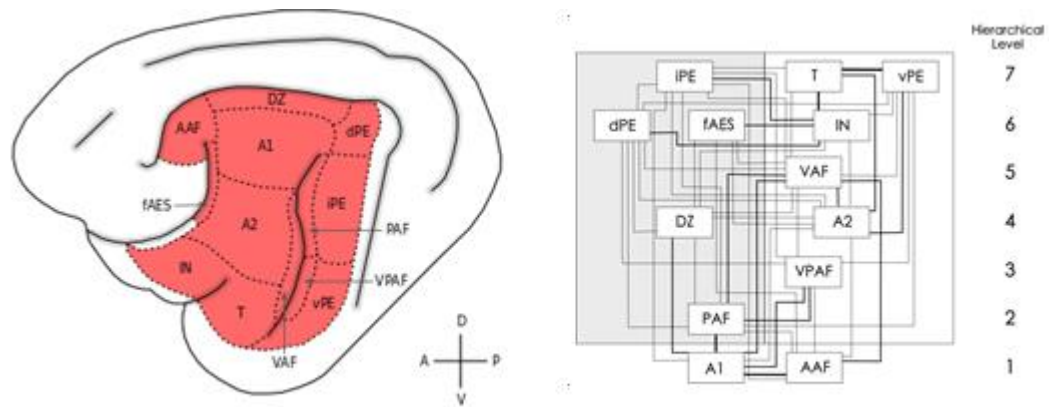


Figure 2-5 The Subregions of the Cat Auditory Cortex and the Processing Hierarchy. Lateral view of the feline brain showing the thirteen subdivisions of the auditory cortex (left) and their arrangement within the auditory processing hierarchy proposed by Lee and Winer (2011; right).

Current Study

Segmenting and ascribing function to specific areas of cortex has been a focus of inquiry for over a century and has become central to the way we understand the organization of the brain's complex networks, and develop therapeutic interventions. While the advent of fMRI has accelerated knowledge in the space, the reliance on functional localizers has limited the scope of inquiry. Accordingly, the current study aims to determine whether patterns of myelin density across the hierarchy of function in auditory cortex might be a useful anatomical biomarker for segmentation in the cat auditory cortex. The cat is an excellent model for auditory cortical work for a number of reasons. First, the feline auditory cortex represents a simplified, tractable version of both the human and monkey auditory cortices (Lomber and Malhotra, 2008). Furthermore, the cat auditory cortex is easily accessible, being exposed on the surfaces of gyri rather than buried within sulci (as occurs in monkeys) (Lomber and Malhotra, 2008). Auditory cues are also highly relevant to cats – in fact, cats have among the best hearing of all mammals (Ryugo and Mennotti-Raymond, 2012). This is reflected anatomically by the large size of the cat auditory cortex, occupying about 20% of cortical volume. Lastly, because of the ease and efficacy of performing sensory systems research in cats, it is a historically well-studied model in not only the auditory, but visual system as well. The breadth of sensory research in cat models facilitates comparisons within and across systems.

I aimed to provide the first qualitative assessment of how patterns of myelination vary by region to determine the extent to which areal borders could be identified by shifts in myelination. To this end, I have generated detailed quantifications of myelin density across regions and cortical depths to test the hypothesis that myelin density is inversely related to the position of a given region within the hierarchy of sound processing. Interest in myeloarchitecture has seen a recent resurgence, due at least in part to technological innovations in myelin-sensitive and non-invasive MRI sequences (De Martino et al. 2015, Aung et al. 2013, Glasser and Van Essen 2011). This thesis provides detailed ground-truth estimates against which non-invasive estimates can be compared and be used to validate myelin's potential as a non-invasive structural biomarker for segmenting auditory cortex.

Chapter 2

3 Methodology

3.1 Tissue Preparation

Two domestic short-haired cats (males, aged 1-2 years) were obtained from a commercial breeding facility (Marshall Bioresources; Waverly, NY). At the time of sacrifice, each animal was anesthetized with ketamine (4 mg/kg, i.m.) and dexdomitor (0.03 mg/kg, i.m.) and a catheter was inserted into the cephalic vein for drug administration. Sodium pentobarbital (40 mg/kg, i.v.) was administered to induce general anesthesia. Heparin (1 mL: an anti-coagulant) and 1% sodium nitrite (1 mL: a vasodilator) were co-administered intravenously. Each animal was then perfused transcardially with physiological saline (1 L), followed by 4% paraformaldehyde (2 L) at a rate of 100 mL/min. To ensure correct orientation for sectioning and inclusion of the entire auditory cortex, the brain was blocked in the coronal plane between Horsley and Clark (1908) levels +18 and -2, before removal from the cranium. To cryoprotect the tissue, each brain was placed serially in 10%, 20%, and 30% (w/v) sucrose solutions until fully submerged. The brains were then cut into six series consisting of 60 μ m coronal sections using a cryostat-microtome (Thermo-Fisher, Waltham, Mass), and each series was stored in ethylene glycol solution at 4 °C. Sections from two series (180 μ m intervals) were stained for myelin using a modified Gallyas Silver Impregnation method (Gallyas 1979, Pistorio et al. 2006, Joseph et al. 2019), and sections from an additional series were processed for neurofilament protein SMI-32 immunoreactivity. All procedures were conducted in accordance with the Canadian Council on Animal Care's Guide to the Care and Use of Experimental Animals and were approved by the University of Western Ontario Animal Use Subcommittee of the University Council on Animal Care.

3.2 SMI-32 Immunohistochemistry

Antibodies sensitive to SMI-32 recognize a non-phosphorylated epitope of neurofilament proteins, which are thought to be necessary for the maintenance of large, myelinated neurons (Ouda et al., 2012). Importantly, SMI-32 is known to be differentially expressed across subregions of the auditory cortex (Mellot et al., 2010), and represents the current gold standard in histologically parcellating auditory cortex (Butler et al., 2016; 2018). In order to visualize patterns of SMI-32 reactivity, sections were removed from ethylene glycol solution and rinsed with 0.1 M physiological buffer (PB; 3 x 5 min). Endogenous peroxidase was blocked with 0.5% hydrogen peroxide in 70% ethanol for 30 minutes, and sections were again rinsed with 0.1 M PB (4 x 5 min). Following this, sections were incubated in normal goat serum (5% NGS in 0.1M PB) for 45 min, and incubated in primary antibody (mouse-anti-SMI-32; 1/2000; Vector Laboratories, Burlingame, CA, USA in 2% NGS in PB) at room temperature overnight. Sections were then rinsed with 0.1 M PB (4 x 5 min) before being incubated in biotinylated secondary antibody (goat anti-mouse IgG; 1/200; Vector Laboratories in 2% NGS in PB) for 30 min. After rinsing with 0.1 M PB (3 x 10 min), sections were incubated with an avidin–biotin–horseradish peroxidase solution (Vectastain Elite ABC, Vector Laboratories) for 90 minutes. Sections were then rinsed with 0.1 M PB (3 x 10 mins), and incubated with a diaminobenzene–nickel chromogen solution for 15 min. After a final series of rinses with 0.1 M PB (3 x 5 min), sections were mounted from 0.01M PB on gelatinized slides, dehydrated via submersion in increasing concentrations of alcohol (50 > 70 > 95 > 100), cleared with HistoClear (3x10 min) and coverslipped.

3.3 Myelin Visualization

Sections stained for the presence of myelinated fibers were removed from ethylene glycol solution and rinsed (3 x 5 minutes) in deionized water. Sections were then submerged for 30 minutes in a 2:1 solution of pyridine and acetic anhydride. Incubated sections were then rinsed in 0.5% acetic acid (3 x 3 minutes) before being submerged in Ammoniacal Silver solution (0.1% ammonium nitrate, 0.1% silver nitrate w/v) for 1 hour, after which

acetic acid washes (3 x 3 minutes) were repeated. Sections were then placed in a developer solution containing equal quantities of 5% sodium carbonate anhydrous (w/v) and a solution of 0.2% ammonium nitrate, 0.2% Silver nitrate, and 1% tungstosilicic acid hydrate (w/v) for 5 min. Following this, sections were rinsed with deionized water (3 x 5 minutes) and bleached in KFeCn solution (0.5% w/v) for 3 min before being rinsed again in deionized water (3 x 5 minutes). This process of development, bleaching, and rinsing was repeated twice to ensure the tissue was well-developed and uniformly stained. At that point, tissue was fixed by submerging in 0.5% NaThioSO₄ for 5 minutes and rinsed thoroughly in deionized water (3x10 minutes) in preparation for mounting (Fig. 1). Sections were mounted from gel alcohol (1% gelatine [w/v] in equal parts deionized water and 95% alcohol), dehydrated via submersion in increasing concentrations of alcohol (50% > 70% > 95% > 100%), cleared with HistoClear (3x10 min) and coverslipped.

3.4 Myelin Quantification

Myelinated fiber length density (MFLD) estimates for each region of the auditory cortex were derived from Gallyas-stained sections using a computerized stereology system consisting of StereoInvestigator software (MBF Bioscience), and a Zeiss AxioImager M2 microscope. First, the boundaries of the 13 auditory cortical areas were derived from SMI-32 stained sections for each animal as described by Mellott and colleagues (9). Additionally, each auditory cortical region was further divided into separate regions of interest (ROIs) comprising layers I-III (superficial), IV (intermediate), and V-VI (deep), for a total of 39 ROIs. The outlines of the 39 ROIs were then superimposed on the adjacent myelin-stained sections from the same animal to define the ROIs within which MFLD estimates would be computed (Figure 2.1).

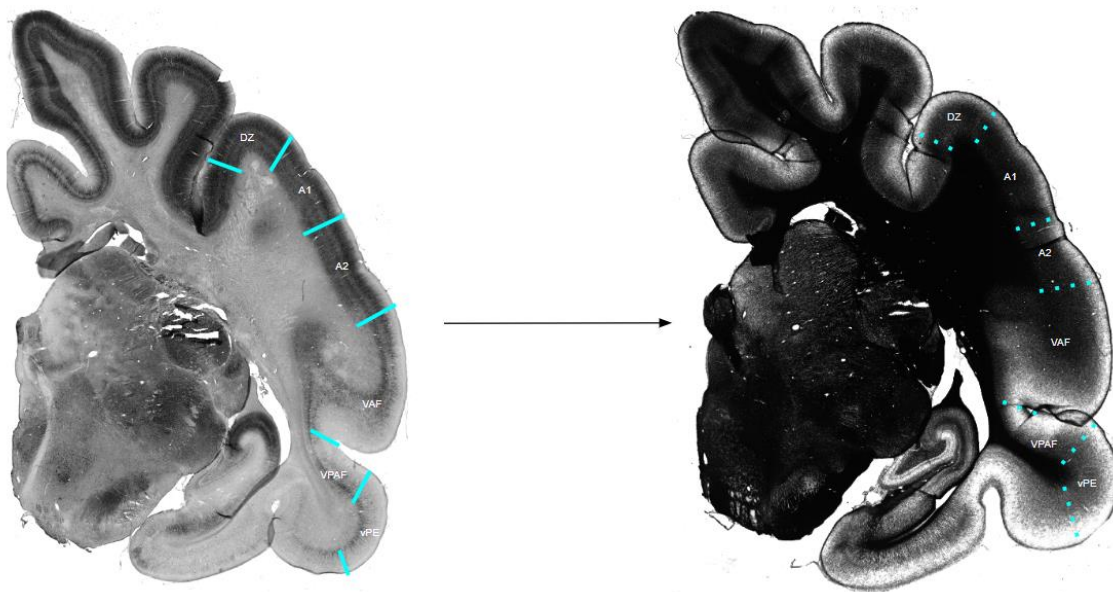


Figure 3-1 Transfer of ROIs from SMI-32 to Myelin-Stained Sections. Areal borders between subregions are defined based on SMI-32 staining pattern as described in the literature. Borders are then superimposed on adjacent myelin-stained sections to interpolate regions of interest (ROIs) in which myelin is to be quantified.

Myelin was quantified using the Spaceballs probe, which is used to estimate the total length of linear biological features as described by Mouton et al. (2002). The Spaceballs probe has been used extensively in several quantitative anatomical studies that involve length estimation of capillaries, axons, dendrites, and myelin (Liu et al. 2011; McNeal et al. 2016; Nikolajsen et al. 2015), and generates length estimates based on the probability that the surface of a spherical probe is intersected by a “line” that is randomly oriented in 3D space of known volume. Specifically, the formula used by the probe to estimate length density is:

$$L_v = 2QA$$

wherein the length of a linear feature per unit volume (L_v) is equal to the number of times that linear feature (Q) passes through a probe of known area (A) multiplied by 2. However, this formula assumes an isotropic interaction between the linear feature and the probe (West, 2018). Prior to the invention of the Spaceballs method, stereological estimates of length required that researchers randomly orient tissue (Baddeley et al. 1986), cut in orthogonal planes (Mattfeldt et al. 1985), or randomly orient flat surface probes on arbitrarily cut tissue (Larsen et al. 1998). However, sectioning in random orientation is often inappropriate; for example, the current study required that tissue be sectioned in a preferred orientation (the coronal plane) in order to reproduce previously observed patterns of SMI-32 labeling and allow for analysis of myelination across the cortical mantle (Mellot et al. 2010). To circumvent this, the Spaceballs workflow superimposes an isotropic, hemispheric virtual probe into a designated volume of tissue in which a linear feature is estimated, thereby ensuring that any interaction between that feature and the surface of the probe is isotropic by definition.

Hemispheric Spaceballs probes were placed in a systematic random fashion to cover the entire ROI on Gallyas-stained tissue, with sampling parameters selected to ensure 70-100 probes would be performed within each ROI across a minimum of 3 sections. In order to extrapolate MFLD estimates to the volume of each ROI, mean mounted section thickness was computed from thickness measures taken at every 5 sampling locations. The analysis was performed under Koehler illumination at 100x. For each ROI, the MFLD was calculated by the StereoInvestigator software according to the equation described above. Finally, the variance was calculated to ensure a coefficient of error below the literature standard (0.1; see Appendix A for CE values). For an exhaustive list of all sampling parameters across both cats, see Appendix B.

3.5 Statistical Analysis

To determine whether myelin density varied systematically by cortical depth across the auditory cortex, a repeated measures ANOVA was computed with region (13 levels; see Figure 1-5) and depth (supragranular, granular, infragranular) as within-subjects factors.

The three ROIs which comprised each cortical subregion varied significantly in volume. Thus, to examine how overall myelin density varied across cortical subregions, weighted MFLD estimates were computed for each subregion by multiplying the MFLD of each ROI by the proportion of the total volume that each ROI within a given subregion comprised. For example, the overall myelin density of A1 was computed as follows:

$$MFLD_{A1Total} = MFLD_{A1Supra} \times \frac{Vol_{A1Supra}}{Vol_{A1Total}} + MFLD_{A1Gran} \times \frac{Vol_{A1Gran}}{Vol_{A1Total}} + MFLD_{A1Infra} \times \frac{Vol_{A1Infra}}{Vol_{A1Total}}$$

A separate repeated measures ANOVA was conducted to determine whether the MFLD differed across cortical subregions using these weighted estimates as a within-subjects factor (13 levels). Pairwise comparisons were further examined using a Tukey's honestly significant difference test (HSD). Finally, a correlation analysis was performed to determine whether the myelin density of auditory cortical subregions was related to their position within the functional hierarchy proposed by Lee and Winer (2011).

Chapter 3

4 Results

The purpose of this investigation was to quantify and compare patterns of myelination across the 13 subregions of the feline auditory cortex to determine how myeloarchitecture changes across cortical depth and position within the functional hierarchy of auditory processing. The presence of measurable areal differences would support the idea that myelin density may be useful in discerning the borders between adjacent cortical regions. This process followed three broad steps: 1) identification of auditory cortical subregions on myelin-stained sections using patterns of SMI-32 reactivity; 2) generation of myelinated fiber length density profiles for each of the 13 auditory subregions, with quantitative estimates generated for each of the supragranular (I-III), granular (IV), and infragranular (V, VI) layers; and 3) statistical comparison of resulting quantitative myelin profiles between adjacent regions to ensure that they differed significantly.

4.1 Myelin Differences Across Anatomical Borders

How patterns of myelination change across the feline auditory cortex has not been previously described. Thus, in order to generate estimates, the borders between subregions of auditory cortex that were visualized using patterns of SMI-32 reactivity (Mellott et al., 2010), were superimposed onto adjacent myelin-stained sections. In addition to defining the subregions within which myelin was to be quantified, patterns of SMI-32 reactivity could also be used to segregate cortex into supragranular, granular, and infragranular layers, based on the near absence of SMI-32 reactivity in the granular layer of cortex (N.B., this approach did not allow for a full layerwise analysis of myelin density, as the patterns of SMI-32 reactivity do not provide clear delineation of the infra/supragranular layers). This permitted observation of the differences in myelin across the prospective regions of interest and their constituent depths. The photomicrographs presented in Figure 3-1 provide a qualitative look at how myelin density changes at areal borders.

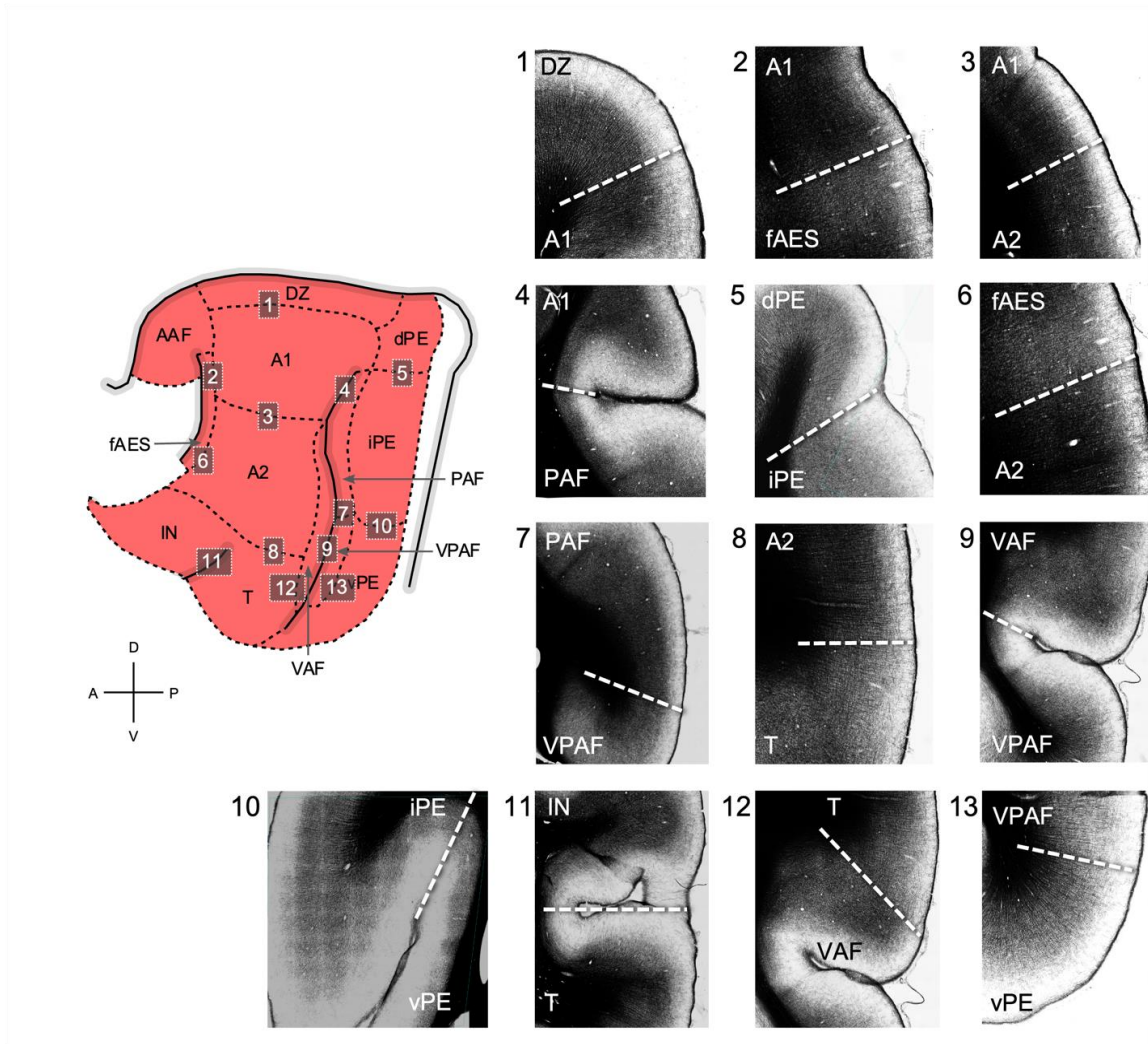


Figure 4-1 Photomicrographs of Auditory Cortical Subregions.

Photomicrographs of auditory cortical subregions showing myelination as visualized using a modified Gallyas silver impregnation protocol and captured using a 40x objective. The numbered panels correspond to the labelled borders shown on the lateral view of the auditory cortex (left). Subregions are labelled and dashed lines show areal borders as defined by SMI-32 reactivity of adjacent sections. Note that, due to the orientation of sectioning, not all borders can be well illustrated.

Figure 3-1 shows the borders between the primary auditory cortex (A1) and the dorsal zone of auditory cortex (DZ; panel 1), the auditory division of the anterior ectosylvian sulcus (fAES; panel 2), and the second auditory cortex (A2; panel 3). A1 was observed to have a higher myelin density than each of these across animals and sections studied, and the borders between A1 and each region were noted to be non-transitional (i.e. a fairly abrupt change in the density of staining). Panel 4 shows the border between A1 and the posterior auditory field (PAF). A1 and PAF are quite similar in their patterns of myelination, with a more transitional border between the two. However, the presence of the posterior ectosylvian sulcus between A1 and PAF is helpful in delineating the two areas.

Panel 6 shows the border between the dorsal and intermediate divisions of the posterior ectosylvian gyrus (dPE and iPE, respectively). dPE was found to be more densely myelinated than iPE, with the difference between the two subregions becoming more apparent as you observe more ventrally in iPE. Accordingly, the dPE/iPE border is considered transitional, with efforts to delineate the two supported by an indentation which extends from the dorsal aspect of the posterior ectosylvian sulcus. Very little change in myelin density can be observed at the border between iPE and the ventral division of the posterior ectosylvian sulcus (vPE; panel 10).

A clear non-transitional border is apparent between A2 and fAES (panel 6), with A2 appearing much more densely myelinated. A2 is also clearly more densely myelinated than the temporal region of auditory cortex (T; panel 8), with the border between the areas appearing non-transitional. Clear borders are evident between the ventral posterior auditory field and PAF (panel 7), the ventral auditory field (VAF; panel 9), and vPE (panel 12). In each case, areas PAF, VAF, and vPE are found to be more densely myelinated than VPAF.

Finally, the insular auditory cortical area (IN) is more myelinated than the temporal area (T panel 11), particularly within deeper lamina. While the border between IN and T is

transitional, its placement is facilitated by the dorsal aspect of the sylvian fissure, which separates the two.

In addition to visualizing how patterns of myelination change at areal borders in auditory cortex, Figure 3-2 provides a qualitative view of how myelin density changes across the dorsal (panel a) and ventral (panel b) streams of the functional hierarchy proposed by Lee and Winer (2011). At a glance, it appears that the patterns observed in the current study are in general accordance with the idea that myelin density is inversely related to the level at which regions reside within such a hierarchical arrangement. A clear outlier, however, is VPAF which, despite being located near the bottom of the ventral auditory stream, appears to be sparsely myelinated relative to other regions of auditory cortex.

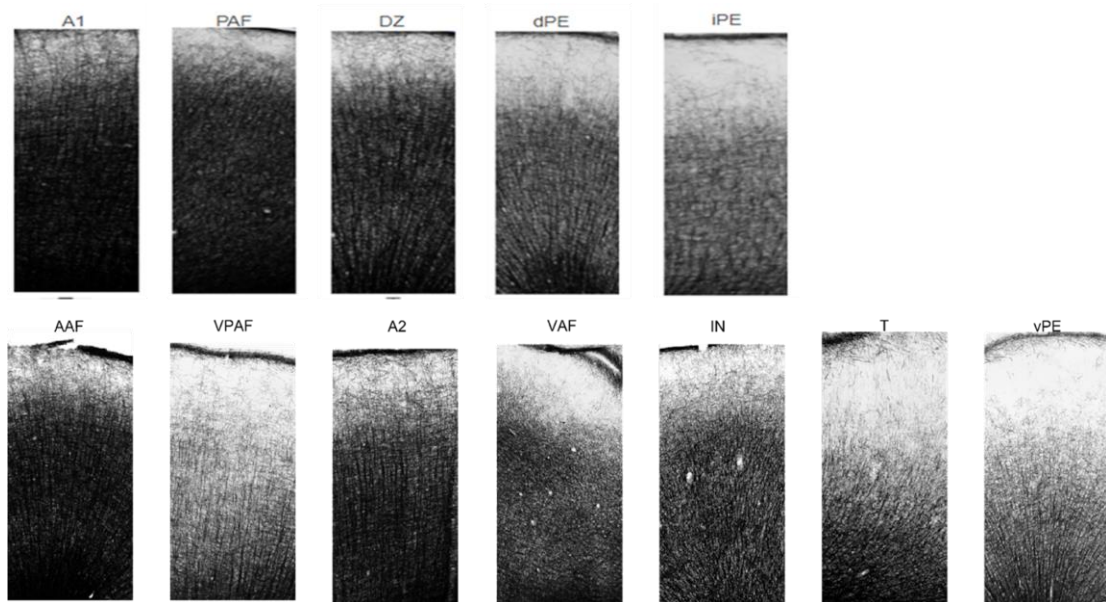


Figure 4-2 Columnar Photomicrographs of Auditory Cortical Subregions.

Photomicrographs of auditory cortical subregions arranged according to their level in the dorsal (A) and ventral (B) processing hierarchies proposed by Lee and Winer (2011). Note: due to its orientation relative to the sectioning plane, the auditory field of the anterior ectosylvian sulcus cannot be well represented in this way, and has been omitted.

4.2 Stereological Quantification of Myelin: Accordance with the Processing Hierarchy, Effect of Depth, and Quantitative Comparisons Between Sub-Regions

Stereology is the process of sampling and counting specific features within a tissue sample using microscopy to generate an estimate of some quantitative parameter. For example, the Spaceballs probe (Mouton et al., 2002) was designed to allow for the generation of length density estimates when quantifying linear features of interest. By virtually embedding an array of hemispheric probes into randomly sampled volumes of tissue, and placing markers where myelinated fibers intersected with the areal borders of those probes, we were able to generate quantitative myelin length density estimates for each of our 39 regions of interest (13 subregions comprising the feline auditory cortex x 3 depths along the thickness of the cortical mantle). These 39 ROIs allowed us to determine whether subregions differed in terms of their total myelin content according to the proposed processing hierarchy and compare the laminar distribution of myelin across subregions.

It has been established that across a broad range of areas, the deepest layers of cortex are the most myelinated, with decreasing myelination as you observe more superficially (Glasser et al. 2014). This can be attributed to the infragranular layers' proximity to the heavily myelinated white matter, intrinsic myelin gradients in the brain, and the infragranular layers' dense thalamocortical connectivity (Slater et al. 2019). That myelin length density changes as a function of cortical depth is apparent in the photomicrographs presented in Figure 3-3. To determine whether these changes reached statistical significance, a repeated measures factorial ANOVA was performed with cortical region (13 areas described above) and depth (supragranular, granular, infragranular) as within-subjects factors. This analysis revealed a significant effect of cortical depth ($F[2,2]=43.46$, $p=0.023$; Figure 3-3). A postdoc Tukey's honestly significant difference (HSD) test revealed that myelin length density was greater in the infragranular layers than in the granular and supragranular layers (both $p_{\text{adj}} < 0.001$), and was greater in the granular layer than in the supragranular layers ($p_{\text{adj}} < 0.001$).

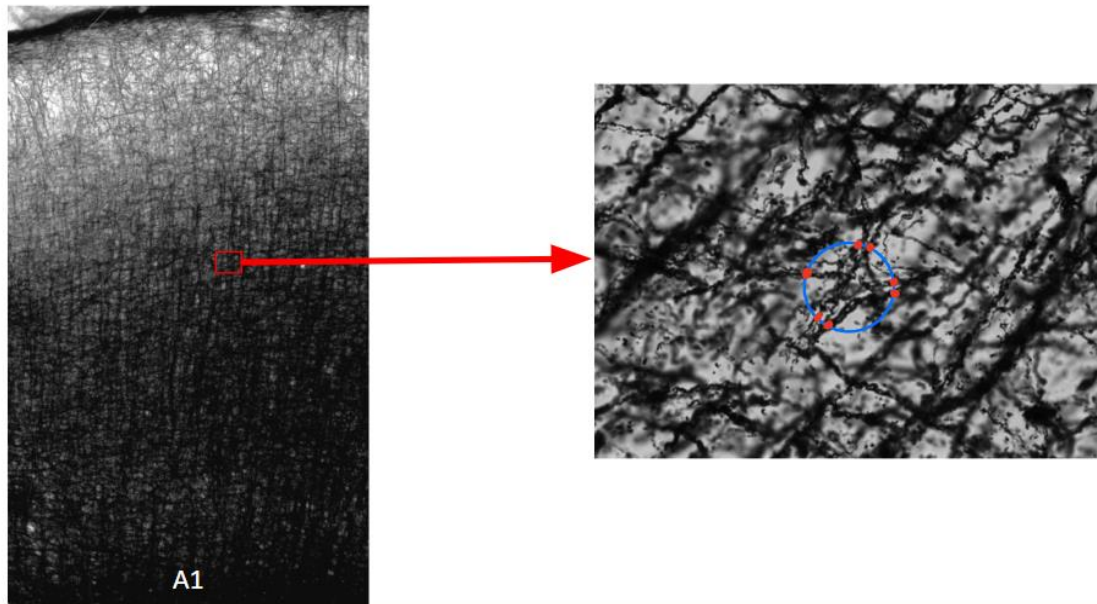


Figure 4-3: A Visual Representation of the Spaceballs Probe. (Left) A photomicrograph of cat primary auditory cortex in which myelin was quantified. (Right) The area enclosed by the red square in the left hand panel magnified using the 100x lens. The blue circle represents the boundary of the hemispheric Spaceballs probe. Red markers denote where in-focus myelinated fibers intersect the boundary of the probe.

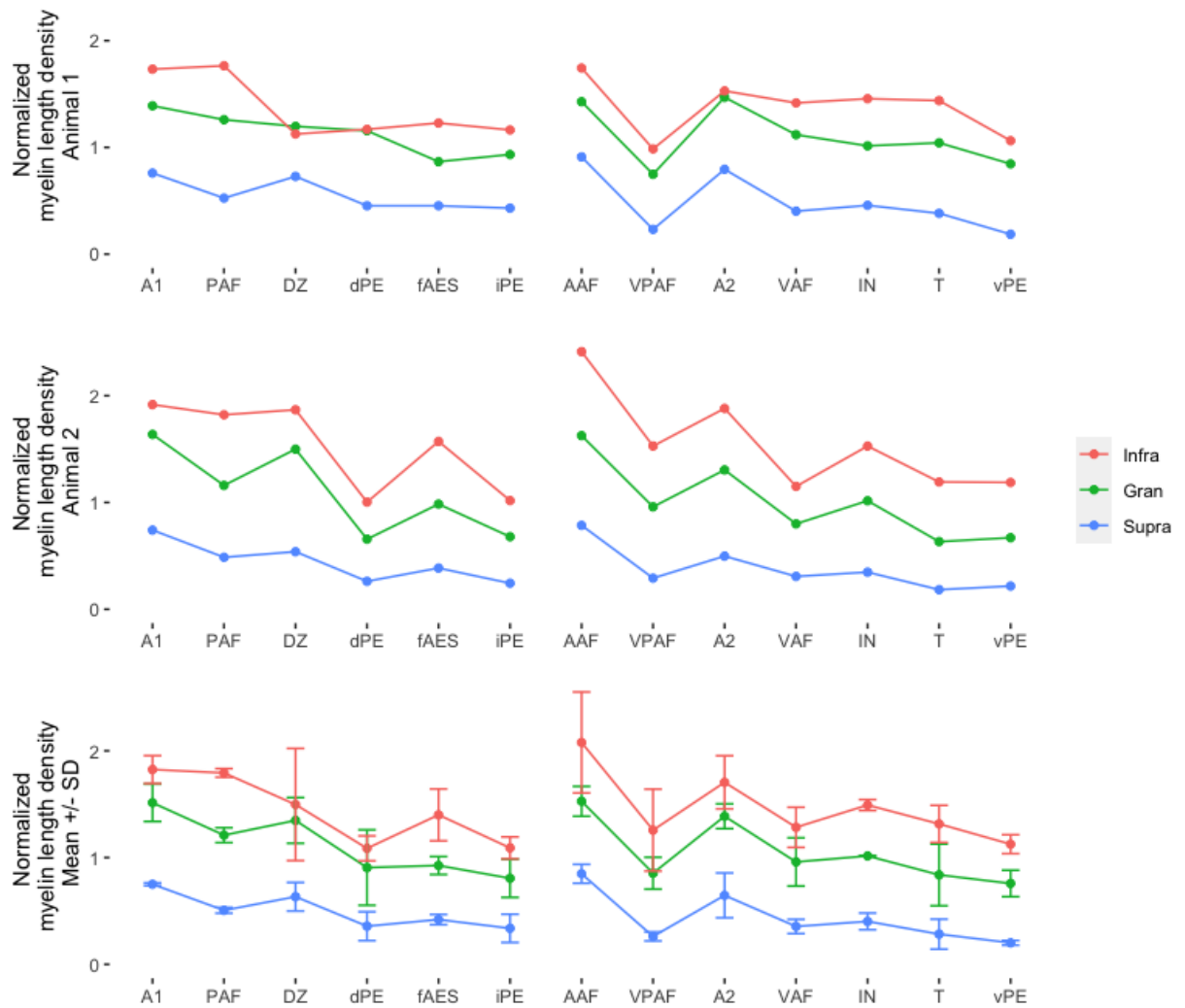


Figure 4-4: Normalized Myelin Length Density Across Two Cats. Myelin length density (MLD) normalized within-animal to mean MLD across regions of interest for animal 1 (A), animal 2 (B), and averaged across both animals (C; mean \pm SD). Data are separated by cortical depth to show MLD in supragranular (blue), granular (green), and infragranular (red) layers. Cortical subregions have been arranged according to the functional hierarchies proposed by Lee and Winer (2011), with the purported dorsal stream at left and ventral stream at right.

No significant interaction was observed between subregion and depth ($F[24,24]=1.018$, $p=0.48$). Thus, a separate repeated-measures ANOVA was performed in which data were collapsed across cortical depth to determine whether statistically significant differences in myelination were observed between cortical subregions (Figure 3-4). Because the three ROIs comprising each cortical subregion (e.g. $A1_{supra}$, $A1_{gran}$, and $A1_{infra}$) were of unequal volume, a weighted myelin length density estimate was computed for each subregion by multiplying the density at each cortical depth by the proportion of the total subregion's volume that comprised the ROI at that depth. This analysis revealed a significant effect of subregion ($F[12,12]=7.612$, $p<0.001$). A follow-up Tukey's HSD test revealed that myelin density was greater in the primary auditory cortex (A1) than in areas dPE, iPE, vPE, VAF, VPAF, and T (all $p_{adj}<0.05$). Additionally, the anterior auditory field (AAF) had higher myelin length density than dPE, iPE, vPE, VAF, VPAF, IN, and T (all $p_{adj}<0.05$). Finally, the second auditory cortex (A2) had higher myelin length density than vPE and VPAF (both $p_{adj}<0.05$).

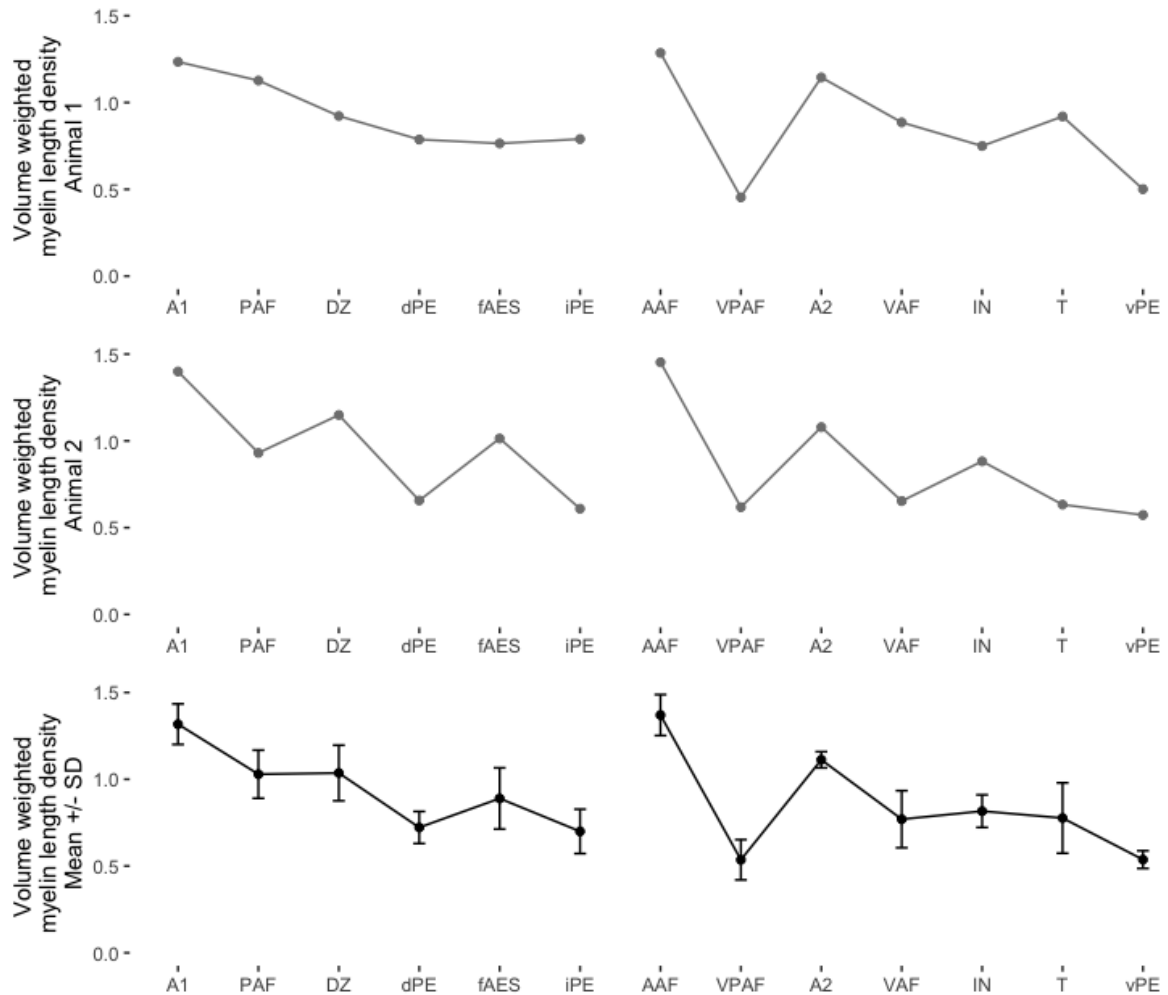


Figure 4-5: Myelin Length Density Collapsed Across Depths Within Subregions. Myelin length density (MLD) in each subregion of auditory cortex collapsed across the three depths sampled. Because regions of interest differed significantly in size, volume-weighted estimates were computed by multiplying the values shown in Figure 3-3 by the proportion of each subregion occupied by each ROI. Data are shown for animal 1 (A), animal 2 (B), and for the average across animals (C; mean \pm SD). Cortical subregions have been arranged according to the functional hierarchies proposed by Lee and Winer (2011), with the purported dorsal stream at left and ventral stream at right.

Dividing our analyses across depths within subregions also allowed us to compare whether - in addition to total myelin content - the distribution of myelin by depth would differ across areas. We wanted to visualize whether differences between regions were driven primarily by differences in specific depths or whether changes were broad and occurred across all depths. Our results from the first two animals imply that changes in myelination between regions occur across all three depths of cortex (Figure 3-3). This change-across-depth pattern was evident in the ventral processing pathways of both animals as well as the dorsal processing pathway of animal 2, though in animal 1 the trend in the dorsal pathway becomes less clear. A notable exception appears to be in the myelin differences that exist between A1 and PAF, two tonotopically organized areas that share a large border and are thought to be sequentially organized along the dorsal stream processing hierarchy. While A1 and PAF have very similar supragranular myelin densities, differences are apparent in the granular and infragranular layer (the granular layer has relatively small volume, thus granular differences contribute less to total variation in myelin than do differences in supragranular and infragranular differences).

Finally, to test the hypothesis that myelin length density is highest in core cortical subregions, and diminishes in higher order cortical areas, a correlation analysis was performed. The position within the hierarchy of auditory cortical processing for each subregion was taken from the arrangement proposed by Lee and Winer (2011: Figure 3-5a). Accordingly, hierarchical position was assigned from a categorical scale ranging from 1 (core subregion) to 7 (highest-order areas). Across the proposed dorsal and ventral streams of auditory processing, a significant negative correlation was observed between myelin length density and hierarchical position ($S=4851.9$, Spearman's $\rho=-0.659$, $p<0.001$; Figure 3-5b).

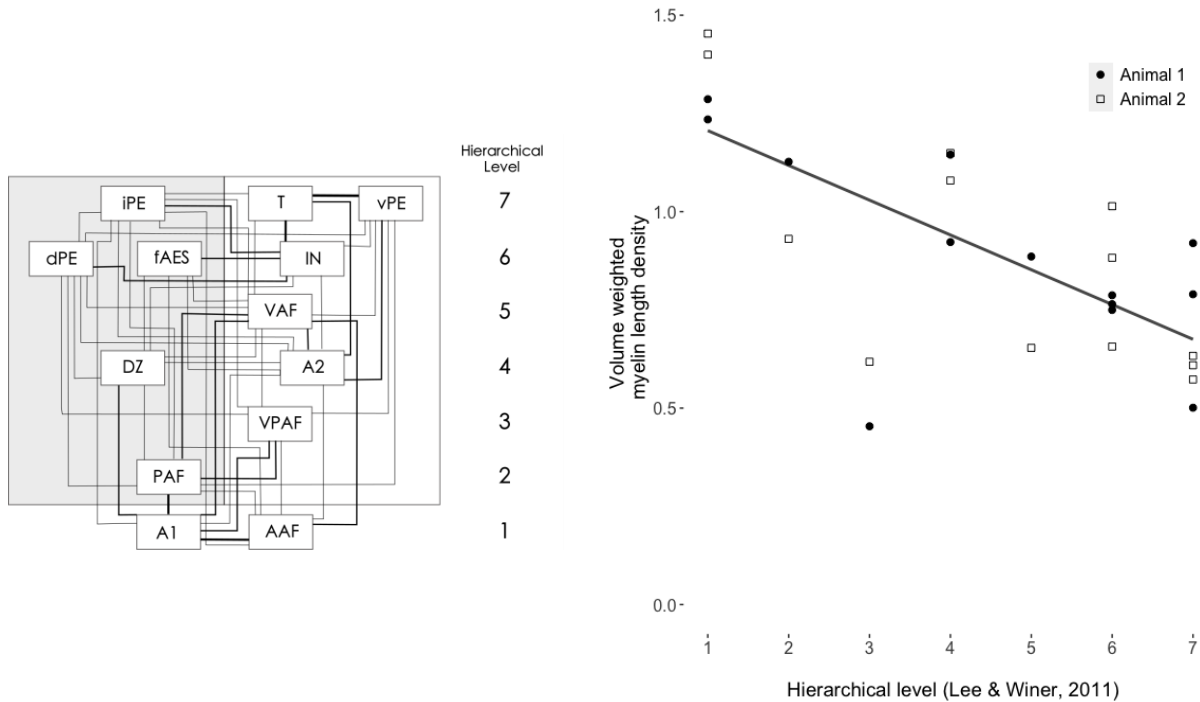


Figure 4-6: Volume Weighted Myelin Length Density vs. Subregion Level on Processing Hierarchy. (A) The hierarchy of the feline auditory cortex as proposed by Lee and Winer (2011). Separate perception and action streams are shown, extending across 7 proposed hierarchical levels beginning with core subregions (A1, AAF) and extending toward higher-order areas. (B) Observed correlation between purported hierarchical level and myelin length density across auditory cortical subregions. Analysis revealed a strong negative correlation (Spearman's $\rho = -0.659$, $p < 0.001$) across animals (animal 1 - filled circles; animal 2 - open squares) suggesting that higher-order subregions are sparsely myelinated compared to core regions.

Chapter 4

5 Discussion

This project sought to quantify the way in which patterns of myelination differ across the feline auditory cortex, and to assess whether myeloarchitecture might serve as a structural biomarker capable of delineating its 13 constituent subregions. Myelin was chosen because 1) previous studies in other models/systems suggested that myelin density could - at minimum - likely resolve core cortical regions from higher-order areas, and 2) because modern neuroimaging techniques exist that purport to be highly sensitive to myelin such that it may be possible to obtain non-invasive myeloarchitecture profiles *in vivo* (Glasser and Van Essen, 2011; Glasser et al. 2014; Moerel et al. 2014; De Martino et al. 2015).

Neuroimaging studies in humans (Glasser et al. 2014; Glasser and Van Essen, 2011) and histological observations made across a number of mammalian species (see Sanides, 1969 for review) have suggested that core, and early unimodal brain areas across sensory cortices (i.e. visual, auditory, and somatosensory cortex) are heavily myelinated, while higher order association regions show significantly lower myelin densities. The functional organization of the feline auditory cortex has been previously described (Lee and Winer, 2011) based on detailed studies of the patterns of thalamic inputs to, and cortical connections between subregions (Lee & Winer 2008a; 2008b). Accordingly, there existed at the outset of the current project, a hierarchy over which a gradient of myelin density was hypothesized to exist. Indeed, the results of the current study largely align with this hierarchy, and are in agreement with previous qualitative observations of how myelin is distributed within sensory cortices.

Here, we present myelin length density estimates for each of 39 regions of interest (13 subregions comprising the feline auditory cortex x 3 depths along the thickness of the cortical mantle). These 39 ROIs provide insight into how subregions differ in terms of their total myelin density, how these differences relate to the position of these subregions within the proposed dual-stream processing hierarchy, and how laminar distributions of myelin compare across subregions.

5.1 Patterns of Myelin Length Density in Auditory Cortex

At low magnification many of the borders between auditory cortical subregions can be identified according to their myelination profiles by simple inspection (as is currently done using SMI-32 [e.g., Butler et al, 2018]). In many cases, areal shifts in myelin can be plainly observed between regions that differ by a single level on the processing hierarchy (See Figure 3-1 for images). At many of these borders, shifts in myelin density were sharp, with little apparent transitional zone. However, borders located within sulci (e.g., IN/T, VAF/VPAF, A1/PAF) were more difficult to localize, with changes in myelin density occurring more gradually.

As expected, there is also a clear myelin density gradient across cortical depth, with far more myelin present in deeper than more superficial layers. However, no significant differences were observed in this laminar distribution across subregions. Thus, the areal myelin density profiles provided here lack the layer-specific differences described for SMI-32 reactivity by Mellott et al. (2010). However, the characteristic myelin density patterns described here, combined with prominent anatomical markers (i.e. gyral/sulcal landmarks) that separate many of the areas, provide a useful means of individuating auditory cortical subregions. Furthermore, myelin based parcellation can be used to discriminate between regions that lie along the posterior ectosylvian gyrus (i.e., areas dPE, iPE, and vPE), which were not included in the descriptions provided by Mellott and colleagues (2010).

5.2 Hierarchical Distribution of Myelin in Auditory Cortex

The feline auditory cortical hierarchy comprises two core areas (AAF, A1), three additional low-level areas that are tonotopically organized (PAF, VPAF, VAF), five higher-order areas that respond to more complex acoustic features (A2, FAES, DZ, IN, T) and the multisensory areas that integrate auditory and non-auditory perceptual cues (dPE, iPE, vPE; Lee and Winer, 2011). Tonotopic areas receive the bulk of their thalamic input from the ventral division of the medial geniculate body (MGB) while non-tonotopic

areas receive thalamic input from the dorsal division (Lee and Winer, 2008a). There is also dense interconnectivity between regions (Lee and Winer, 2008b; Lee and Winer, 2011). Additionally, the subregions of auditory cortex are thought to comprise two parallel streams dedicated to processing cues related to sound location and identity. In addition to differing patterns of anatomical connectivity, the dual stream hypothesis has been supported by functional data. For example, deactivation of A1, PAF, FAES or DZ leads to deficits in auditory localization, but not discrimination (Malhotra et al., 2004; Malhotra et al. 2008), while AAF deactivation impairs auditory discrimination, but not localization (Lomber and Malhotra, 2008).

Previous studies have suggested that within sensory cortices, a myelination gradient exists such that core regions are myelinated earlier and to a greater extent than higher-order areas. Accordingly, the current study observed that the core regions of the feline auditory cortex (A1/AAF) were the most heavily myelinated areas studied. Indeed, even with a sample size of two animals, these core areas were found to be significantly more myelinated than many other areas of the auditory brain. Moreover, MFLD estimates across subregions were significantly correlated with the position of those regions within the functional hierarchy proposed by Lee and Winer (2011), suggesting a linear decline in myelin density as you ascend the auditory processing pathways.

There are a few possible explanations for the inverse relationship between hierarchical position and myelin density. First, because they comprise the principle thalamic targets within the complex branching streams of sound processing (e.g., 42 % of the inputs to A1 are thalamic in origin compared to only 29% in A2; Chabot et al., 2015; Butler et al., 2018), regions at the core of the processing hierarchy are in receipt of a great deal more auditory input than higher-order regions, which process only a subset of that information. Additionally, these thalamocortical connections are established earlier in development than the cortico-cortical projections which dominate the inputs to higher-order auditory cortical areas. Since axons in regions that are myelinated early tend also to be myelinated more rapidly and more completely (Stadelman et al. 2019), the increased myelin density observed in core areas of the auditory cortex may reflect an abundance of early inputs to those areas. This myelin gradient across the functional hierarchy is also in accordance

with observations that higher-order sensory brain regions show more evidence of experience-dependent plasticity than core areas. Since factors associated with axonal myelination are known to inhibit axonal growth and formation (McGee et al. 2005; Glasser et al. 2014; Kapfhammer and Schwab, 1994), it is unsurprising that core areas are more heavily myelinated, show little to no response to nonauditory stimuli, and show little evidence of reorganization following sensory loss (Stewart and Starr, 1970; Kral et al. 2003; Lomber et al. 2010; Berger et al. 2017). It has been noted that myelination of core sensory areas may ensure these regions can continue to perform their lower-order sensory functions, while higher-order regions may benefit from a more dynamic response of the structure and function (Glasser et al. 2014). Indeed, some of the subregions shown to be sparsely myelinated in our data (e.g., DZ, FAES) have been previously shown to readily take on visual and/or somatosensory functions following hearing loss (Land et al., 2016; Lomber et al. 2010; Meredith et al. 2011; Clemo et al. 2016). While little functional reorganization has been documented in lower-level regions, responses to somatosensory and visual stimuli have been observed following hearing loss in AAF - the most myelinated of the auditory cortical subregions according to our estimates (Meredith and Lomber, 2011). This may have something to do with the fact that AAF shares an extended border with non-auditory brain regions, while other lower-level regions (e.g. A1, PAF) are bounded by other auditory cortical areas.

Although the data presented here largely aligned with our predictions, the ventral posterior auditory field (VPAF) was a notable outlier in our analyses. According to the hierarchy proposed by Lee and Winer (2011), VPAF is a relatively low-level region (VPAF was ascribed a level '3' in our discretized analysis; see Figure 3-5). VPAF is considered to lie between AAF and A2 in the ventral auditory pathway due to its tonotopic organization (a typical feature of low-level auditory cortical areas; (Reale and Imig, 1980; Hall and Lomber, 2015) and a pattern of dense thalamocortical input and reciprocal connectivity with the core auditory areas (Lee and Winer, 2008a; Lee and Winer, 2008b; Lee and Winer, 2011). Despite this, VPAF was found to have a very low myelin length density in the current analysis, with much less myelin than many areas that exist above it in the processing hierarchy. It is possible that the Gallyas stain may have poorly penetrated VPAF, as this region is often located within a sulcus which generally

stain lighter than other areas. However, the current study is not the first to note that VPAF differs significantly from other core and core-adjacent areas (Hall and Lomber, 2015; Schreiner and Urbas, 1988). The functions of VPAF have not yet been clearly defined; it could be that VPAF requires a higher degree of adaptability, or may play a supportive role to other lower-order areas. Moreover, it is possible that VPAF may have been misclassified in the processing hierarchy. It is worth noting, however, that VPAF is anatomically segregated from the other tonotopic core and core-adjacent regions, and is located near the posteroventral pole of auditory cortex. As is clear in Figure 4-1, the spatial arrangement of myelin densities in auditory cortex creates an arrangement that closely resembles a densely myelinated core that is surrounded by a belt of areas with reduced myelin density, and a subsequent parabelt where further reductions in myelin density are apparent. This creates an antero-posterior gradient wherein anteriorly located areas are more myelinated than those located posteriorly, and a dorso-ventral gradient wherein dorsal regions are more heavily myelinated than ventral areas. Accordingly, these spatial gradients of myelin density may also account for the low myelin density of VPAF relative to other tonotopic areas. While this is a plausible explanation for the differences between VPAF and other core regions, it does not fully explain why VPAF is among the least myelinated of all 13 cortical areas studied - even those more ventrally or posteriorly located *and* higher on the processing hierarchy. VPAF should be studied in the future to elucidate the reasons behind its sparse myelination profile and contextualize them within the processing hierarchy, as well as evaluate its contribution to crossmodal plasticity in the deaf auditory cortex.

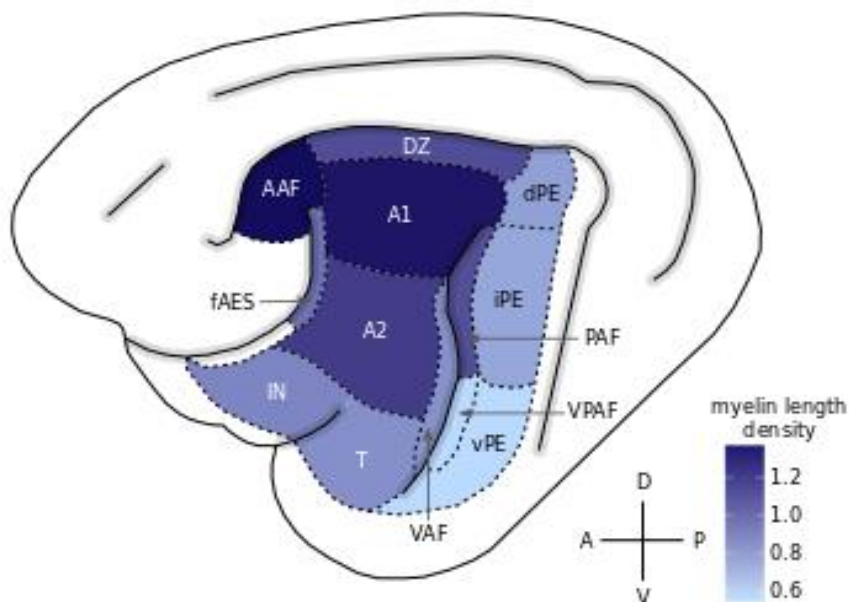


Figure 5-1: Lateral View of Cat Brain With Myelin Length Density Heat Map.

Average normalized myelin length density across both animals superimposed on a lateral view of the cat brain showing the 13 subregions of auditory cortex. Most myelinated regions are dark purple and least myelinated are light blue. Apparent are the strong dorsoventral and anteroposterior myelin gradients (high → low).

5.3 Basis for Cortical Delineation Based on Myeloarchitecture

This project sought to describe the differences in patterns of myelination across the 13 different subregions of cat auditory cortex, and to consider whether these differences might establish myeloarchitecture as a useful and reliable biomarker on which cortical subregions might be delineated. With two animals examined, our analysis revealed myelin density was greater in the primary auditory cortex (A1) than in areas dPE, iPE, vPE, VAF, VPAF, and T (all $p_{adj} < 0.05$). Additionally, the anterior auditory field (AAF) had higher myelin length density than dPE, iPE, vPE, VAF, VPAF, IN, and T (all

$p_{\text{adj}} < 0.05$). Furthermore, the second auditory cortex (A2) had higher myelin length density than vPE and VPAF (both $p_{\text{adj}} < 0.05$). With the exception of VPAF, all of these results are in line with the proposed functional hierarchy in auditory cortex. These marked areal differences suggest that, as predicted, myelin density may be useful in delineating cortical subregions. This is in accordance with existing human neuroimaging studies that have discriminated between core and non-core areas of visual (Glasser and Van Essen, 2011) and auditory cortices (De Martino et al. 2015). Whether similar non-invasive approaches can be applied to delineate feline auditory cortex, and to provide more fine-grained discriminations between subregions remains to be seen.

It is worth noting that while the current study examined all pairwise comparisons of myelin density across brain areas, delineating auditory cortex really only requires significant differences between anatomically adjacent regions. For example, while the observed differences between AAF and dPE/iPE/vPE provide a useful proof-of-concept, these areas are anatomically segregated from one another, and do not share a border. Unfortunately, because auditory cortical subregions appear to cluster into core, belt, and parabelt-like structures (Figure 4-1), many regions that are close or share a border are similarly myelinated. Accordingly, the only significant difference found between two cortical areas that share a border is that between A1 and dPE. However, with an increased sample size, there is reason to believe that at least some adjacent areas will differ with regards to their myelin density. In particular, the borders between A1, A2, PAF and AAF and their surrounding areas, and the border between DZ and dPE may be discernable with additional data. Unfortunately, delineating areas at the ventral and posterior limits of auditory cortex may prove to be more difficult. Specifically, very little difference in myelin density was observed between regions along the posterior ectosylvian gyrus (dPE/iPE/vPE), between areas IN and T, and between areas vPE and VPAF differences.

Collecting myelin density estimates from more animals will help to provide more conclusive results - particularly aimed at delineating cortical regions that share a border. However, even in the absence of robust statistically significant differences, the current data provide detailed estimates of myelin density for all 13 auditory subregions, and provide ground-truth histological quantification against which other attempts to quantify

myelination (both non-invasive and invasive) can be compared. Furthermore, the current work demonstrates that while depth is significantly correlated with myelin content (infragranular layers are more myelinated than the granular layer, which is more myelinated than supragranular layers), the difference in myelination across subregions is consistent across cortical depth. This suggests that future work may not require layerwise specificity, which would handily reduce the amount of time needed to perform our analyses.

5.4 Limitations

5.4.1 Limitations in Sample Size

The relatively small number of subjects ($n = 2$) limits the conclusions that can be drawn from the data collected. Unfortunately, animal acquisition, histological processing, and generation of stereological estimates is a time intensive process that was further delayed by the ongoing pandemic. Still, the data collected from the first two animals demonstrates replicability of myelin density estimates, and yielded significant effect of depth on myelination, the correlation between myelin quantity and position on the processing hierarchy, and significant differences between several core and non-core regions. In the near future we intend to add data from a third animal that will further clarify these relationships.

5.4.2 Methodological Limitations

The Spaceballs probe was designed to generate quantitative estimates of the total length of myelinated fibers that transits a given volume of tissue. The Spaceballs probe does *not* consider other factors that might affect the total volume of myelin within the probe space, including the width of the fibers that comprise the length totals computed by the probe. Thus, while the present study provides highly detailed estimates of fiber length density, there are other approaches that might yield complementary estimates of myelin volume.

Furthermore, in regions of interest that are densely myelinated, the Spaceballs probe could possibly underestimate myelin density. In the sparsely myelinated regions, it is

easy to visualize and denote the points at which all myelinated fibers intersect with the probe boundary. However, in the most densely myelinated regions (e.g., A1, AAF), individual fibers are more difficult to resolve, and it can become difficult to see thin myelinated fibers that may be occluded by thicker axons.

Lastly, the degree to which fibers are stained using the modified Gallyas protocol can vary from run to run such that some anatomists suggest running all the tissue to be used for a project at the same time, to limit the amount of variation observed between animals. This was not feasible for the current project; however, MFLD estimates were normalized within each animal so that differences in staining intensity had minimal effect.

Finally, while a secondary aim of the current study was to determine whether myelin length density might be a useful biomarker for non-invasive approaches to cortical parcellation. While the current study revealed reliable regional differences, it remains to be seen whether these differences will be sufficient to be replicated using, for example, myelin sensitive MRI sequences. That said, the current study provides detailed estimates against which these novel and non-invasive approaches can be compared.

5.5 Future Directions

The successful development of anatomical biomarkers of the boundaries between auditory cortical subregions will address a significant gap in our ability to identify and ascribe functions to distinct regions of the brain using non-invasive approaches. Moreover, these biomarkers will allow for the localization of subregions in the absence of a functional localizer scan, which will allow these regions to be identified and studied even following damage or sensory loss. Combining MRI-based measures of brain activity with structural atlases based on region-specific patterns of myelination and anatomical landmarks, will improve the resolution of spatial estimates.

Future work should seek to replicate the current study in animals with early-onset hearing loss to examine how patterns of cortical myelination are altered by auditory deprivation, and determine to what extent the patterns presented here are replicated in a sample of deaf

animals. Additionally, anatomical estimates could be compared to estimates derived from myelin-sensitive MRI scans to determine which measures best correlated with histological length density estimates, and validate these scans as a means of accurately localizing subregions of auditory cortex (Goubran et al. 2013).

5.6 Conclusion

The current study provides preliminary evidence of the ability of myelin to delineate the 13 subregions of the feline auditory cortex. The use of myelin to parcellate the cortex is not a novel concept - in fact it was first proposed over a century ago (Nieuwenhuys, 2013; Vogt and Vogt 1911). However, myelin-based segmentation has seen a resurgence in the literature, largely as a result of novel non-invasive neuroimaging sequences that purport to be sensitive to the density and direction of myelinated fibers. The current study confirms the presence of a myelin gradient whereby myelin density falls off linearly with ascending position within the proposed hierarchy of function. In addition, the patterns of myelin density observed appear in accordance the suggestion that auditory cortex is comprised of a series of core regions that are surrounded by belt and parabelt regions. Indeed, this geographical organization may in large part explain the observation that VPAF does not conform well to the hierarchical gradient. The regional analyses presented here suggest that, at minimum, core regions can be easily delineated from higher-order areas. However, the addition of more data may further improve the utility of myelin density estimates in resolving areal boundaries. Ultimately, the data collected in this project align with the auditory processing hierarchy proposed by Lee and Winer (2011), and support the idea that the areas that have been observed to undergo a greater degree of experience-dependent plasticity are also more sparsely myelinated. Ultimately, by establishing and validating myelin as a useful biomarker for cortical parcellation, we hope to be able to non-invasively describe the brain networks that underlie complex human behaviours, examine how these brain areas are shaped by developmental experience, and determine how and where aberrant anatomy and/or functions may give rise to complex disease etiologies.

References

- Annese, J. (2009). In Retrospect: Brodmann's brain map. *Nature*, 461(884)
- Aung, W. Y., Mar, S., & Benzinger, T. L. (2013). Diffusion tensor MRI as a biomarker in axonal and myelin damage. *Imaging in medicine*, 5(5), 427–440.
- Baddeley, A. J., Gundersen, H. J., and Cruz-Orive, L. M. (1986). Estimation of surface area from vertical sections. *J. Microsc.* 142, 259–276.
- Berger, C., Kühne, D., Scheper, V., & Kral, A. (2017). Congenital deafness affects deep layers in primary and secondary auditory cortex. *The Journal of comparative neurology*, 525(14), 3110–3125.
- Bernard J. Slater, Stacy K. Sons, Georgiy Yudintsev, Christopher M. Lee, Daniel A. Llano. (2019). Thalamocortical and Intracortical Inputs Differentiate Layer-Specific Mouse Auditory Corticocollicular Neurons. *Journal of Neuroscience*, 39(2) 256-270.
- Broca, P. (1865). Sur le siège de la faculté du langage articulé. *Bulletins et Mémoires de la Société d'Anthropologie de Paris*, 6(1), 377-393.
- Brody BA, Kinney HC, Kloman AS, Gilles FH. Sequence of central nervous system myelination in human infancy. I. An autopsy study of myelination. (1987). *J Neuropathol Exp Neurol.* 46(3), 283-301.
- Butler, B.E., Chabot, N., & Lomber, S.G. (2016). Quantifying and comparing the pattern of thalamic and cortical projections to the posterior auditory field in hearing and deaf cats. *Journal of Comparative Neurology*, 524(13), 2623-2642.
- Butler, B.E., de la Rua, A., Ward-Able, T., & Lomber, S.G. (2018). Cortical and thalamic connectivity to the second auditory cortex is resilient to the onset of deafness. *Brain Structure and Function*, 223(2), 819-835.
- Carrasco, A, Lomber, SG. (2009a). Differential modulatory influences between primary auditory cortex and the anterior auditory field. *J Neurosci*, 29, 8350-8362.
- Chabot N, Butler BE, Lomber SG. (2015). Differential Modification of Cortical and Thalamic Projections to Cat Primary Auditory Cortex Following Early- and Late-Onset Deafness. *J Comp Neurol.* 523(15), 2297-320.

- Clemo HR, Lomber SG, Meredith MA. (2016). Synaptic Basis for Cross-modal Plasticity: Enhanced Supragranular Dendritic Spine Density in Anterior Ectosylvian Auditory Cortex of the Early Deaf Cat. *Cereb Cortex*, 26(4), 1365-76.
- C. M. Karns, C. Stevens, M. W. Dow, E. M. Schorr, and H. J. Neville. (2017). Atypical White-Matter Microstructure in Congenitally Deaf Adults: A Region of Interest and Tractography Study Using Diffusion-Tensor Imaging. *Hearing Research*, 343, 72-82,
- De Martino, F., Moerel, M., Xu, J., van de Moortele, P. F., Ugurbil, K., Goebel, R., Yacoub, E., & Formisano, E. (2015). High-Resolution Mapping of Myeloarchitecture In Vivo: Localization of Auditory Areas in the Human Brain. *Cerebral cortex*, 25(10), 3394–3405.
- Felice T. Sun, Lee M. Miller, Ajay A. Rao, Mark D'Esposito. (2007). Functional Connectivity of Cortical Networks Involved in Bimanual Motor Sequence Learning. *Cerebral Cortex*, 17(5), 1227–1234.
- Gallyas F.(1979). Silver staining of myelin by means of physical development. *Neurol Res*, 1(2), 203-209.
- Glasser, M. F., & Van Essen, D. C. (2011). Mapping human cortical areas in vivo based on myelin content as revealed by T1- and T2-weighted MRI. *J Neurosci*, 31(32), 11597–11616.
- Glasser, M. F., Goyal, M. S., Preuss, T. M., Raichle, M. E., & Van Essen, D. C. (2014). Trends and properties of human cerebral cortex: correlations with cortical myelin content. *NeuroImage*, 93 Pt 2, 165–175.
- Glover G. H. (2011). Overview of functional magnetic resonance imaging. *Neurosurgery clinics of North America*, 22(2), 133–vii.
- Goubran, M., Crukley, C., de Ribaupierre, S., Peters, T.M., and Khan, A.R. (2013). Image registration of ex-vivo MRI to sparsely sectioned histology of hippocampal and neocortical temporal lobe specimens. *Neuroimage*. 83. 770-781.
- Hackett, TA. (2011). Information flow in the auditory cortical network. *Hear Res*, 271, 133-146.
- Hagiwara, A., Hori, M., Kamagata, K., Warntjes, M., Matsuyoshi, D., Nakazawa, M., Ueda, R., Andica, C., Koshino, S., Maekawa, T., Irie, R., Takamura, T., Kumamaru, K. K., Abe, O., & Aoki, S. (2018). Myelin Measurement: Comparison Between Simultaneous Tissue

- Relaxometry, Magnetization Transfer Saturation Index, and T1w/T2w Ratio Methods. *Scientific reports*, 8(1), 10554.
- Hall AJ, Lomber SG. (2015). High-field fMRI reveals tonotopically-organized and core auditory cortex in the cat. *Hear Res*, 325, 1-11.
- Heffner HE. (1987). Ferrier and the study of auditory cortex. *Arch Neurol*, 44(2), 218-21.
- Henkelman RM, Stanisz GJ, Graham SJ. (2001). Magnetization transfer in MRI: a review. *NMR Biomed*, 14(2), 57-64.
- Hofstetter S., Tavor I., Moryosef S.T., Assaf Y. (2013). Short-term learning induces white matter plasticity in the fornix. *J Neurosci*. 33, 12844–12850.
- Horsley V, Clark RH. (1908). The structure and function of the cerebellum examined by a new method. *Brain*, 31, 45-124.
- Huettel SA, Song AW, McCarthy G. (2014). *Functional Magnetic Resonance Imaging*, 3rd Edition. Oxford University Press, London UK
- Joseph S, Werner HB, Stegmüller J. (2019). Gallyas Silver Impregnation of Myelinated Nerve Fibers. *Bio Protoc*. 9(22).
- Kaller, M. S., Lazari, A., Blanco-Duque, C., Sampaio-Baptista, C., & Johansen-Berg, H. (2017). Myelin plasticity and behaviour-connecting the dots. *Current opinion in neurobiology*, 47, 86–92.
- Kao, CH., Khambhati, A.N., Bassett, D.S. et al. (2020). Functional brain network reconfiguration during learning in a dynamic environment. *Nat Commun* 11, 16(82).
- Kapfhammer J. P., Schwab M. E. (1994). Increased expression of the growth-associated protein GAP-43 in the myelin-free rat spinal cord. *Eur. J. Neurosci*. 6, 403–411.
- Karl Zilles. (2018). Brodmann: a pioneer of human brain mapping—his impact on concepts of cortical organization. *Brain*, 141(11), 3262–3278.
- Kinney HC, Brody BA, Kloman AS, Gilles FH. (1988). Sequence of central nervous system myelination in human infancy. II. Patterns of myelination in autopsied infants. *J Neuropathol Exp Neurol*. 47(3), 217-34.
- Kolasa, M., Hakulinen, U., Brander, A., Hagman, S., Dastidar, P., Elovaara, I., & Sumelahti, M. L. (2019). Diffusion tensor imaging and disability progression in multiple sclerosis: A 4-year follow-up study. *Brain and behavior*, 9(1).

- Kral A, Schroder JH, Klinke R, Engel AK. (2003). Absence of cross-modal reorganization in the primary auditory cortex of congenitally deaf cats, *Exp Brain Res*, 153, 605-613.
- Larsen, J. O., Gundersen, H. J., and Nielsen, J. (1998). Global spatial sampling with isotropic virtual planes: estimators of length density and total length in thick, arbitrarily orientated sections. *J. Microsc.* 191, 238–248.
- Land R, Baumhoff P, Tillein J, Lomber SG, Hubka P, Kral A. (2016). Cross-Modal Plasticity in Higher-Order Auditory Cortex of Congenitally Deaf Cats Does Not Limit Auditory Responsiveness to Cochlear Implants. *J Neurosci.* 36(23),6175-85.
- Lazari A, Lipp I. (2021). Can MRI measure myelin? Systematic review, qualitative assessment, and meta-analysis of studies validating microstructural imaging with myelin histology. *Neuroimage.* 230, 117744.
- Lee, C. C., & Winer, J. A. (2008a). Connections of cat auditory cortex: I. Thalamocortical system. *The Journal of comparative neurology*, 507(6), 1879–1900.
- Lee, CC, Winer, JA. (2008b). Connections of cat auditory cortex: III. Corticocortical system. *J Comp Neurol*, 507, 1920-1943.
- Lee, CC, Winer, JA, (2011). Convergence of thalamic and cortical pathways in cat auditory cortex. *Hear Res*, 274, 85-94.
- Lisman J, Cooper K, Sehgal M, Silva AJ. (2018). Memory formation depends on both synapse-specific modifications of synaptic strength and cell-specific increases in excitability. *Nat Neurosci.* 21(3), 309-314.
- Litwin-Kumar, A., Doiron, B. (2014). Formation and maintenance of neuronal assemblies through synaptic plasticity. *Nat Commun* 5, 53(19).
- Liu, Y., Lee, M. K., James, M. M., Price, D. L., Borchelt, D. R., Troncoso, J. C., et al. (2011). Passive (amyloid- β) immunotherapy attenuates monoaminergic axonal degeneration in the A β PPswe/PS1dE9 mice. *J. Alzheimers Dis.* 23, 271–279.
- Logothetis, N. (2008). What we can do and what we cannot do with fMRI. *Nature*, 453, 869–878.
- Lomber SG, Meredith MA, Kral A. (2010). Cross-modal plasticity in specific auditory cortices underlies visual compensations in the deaf, *Nat Neurosci*, 13, 1421-1427.
- Lomber, S., Malhotra, S. (2008). Double dissociation of 'what' and 'where' processing in auditory cortex. *Nat Neurosci*, 11, 609–616.

- Lutti A, Dick F, Sereno MI, Weiskopf N. (2014). Using high-resolution quantitative mapping of R1 as an index of cortical myelination. *Neuroimage*, 93 Pt 2, 176-88.
- MacKay AL, Laule C. (2016). Magnetic Resonance of Myelin Water: An in vivo Marker for Myelin. *Brain Plast*, 2(1), 71-91.
- MacKay AL, Vavasour IM, Rauscher A, Kolind SH, Mädler B, Moore GR, Traboulsee AL, Li DK, Laule C. (2009). MR relaxation in multiple sclerosis. *Neuroimaging Clin N Am*, 19(1), 1-26.
- Malhotra, S, Hall, AJ, Lomber, SG. (2004). Cortical control of sound localization in the cat: Unilateral cooling deactivation of 19 cerebral areas. *J Neurophysiol*, 92, 1625-1643.
- Malhotra, S, Lomber, SG. (2007). Sound localization during homotopic and heterotopic bilateral cooling deactivation of primary and nonprimary auditory cortical areas in the cat. *J Neurophysiol*, 97, 26-43.
- Malhotra, S, Stecker, GC, Middlebrooks, JC, Lomber, SG. (2008). Sound localization deficits during reversible deactivation of primary auditory cortex and/or the dorsal zone. *J Neurophysiol*, 99, 1628-1642.
- Mattfeldt, T., Möbius, H. J., and Mall, G. (1985). Orthogonal triplet probes: an efficient method for unbiased estimation of length and surface of objects with unknown orientation in space. *J. Microsc.* 39, 279–289.
- MBF Biosciences. Spaceballs.
https://www.mbfbioscience.com/help/si11/Content/SI_SPECIFIC/Probes/Spaceballs.htm
- MBF Biosciences. Stereology. <https://www.mbfbioscience.com/stereology>
- McGee, A. W., Yang, Y., Fischer, Q. S., Daw, N. W., & Strittmatter, S. M. (2005). Experience-driven plasticity of visual cortex limited by myelin and Nogo receptor. *Science*, 309(5744), 2222–2226.
- McNeal, D. W., Brandner, D. D., Gong, X., Postupna, N. O., Montine, T. J., Keene, C. D., et al. (2016). Unbiased stereological analysis of reactive astrogliosis to estimate age-associated cerebral white matter injury. *J. Neuropathol. Exp. Neurol*, 75, 539–554.
- Mellott JG, Van der Gucht E, Lee CC, Carrasco A, Winer JA, Lomber SG. (2010). Areas of cat auditory cortex as defined by neurofilament proteins expressing SMI-32. *Hear Res*. 267(1-2) ,119-36.

- Meredith MA, Kryklywy J, McMillan AJ, Malhotra S, Lum-Tai R, Lomber SG. (2011). Crossmodal reorganization in the early deaf switches sensory, but not behavioral roles of auditory cortex. *Proc Natl Acad Sci USA*, 108, 8856-8861.
- Meredith MA, Lomber SG. (2011). Somatosensory and visual crossmodal plasticity in the anterior auditory field of early-deaf cats. *Hear Res*. 280(1-2), 38-47.
- Millett D. (1998). Illustrating a revolution: an unrecognized contribution to the golden era of cerebral localization. *Notes Rec R Soc Lond*. 52(2), 283-305.
- Mishkin, M, Ungerleider, LG, Macko, KA, (1983). Object vision and spatial vision - 2 cortical pathways. *Trends Neurosci*, 6, 414-417.
- Moerel M, De Martino F and Formisano E (2014) An anatomical and functional topography of human auditory cortical areas. *Front. Neurosci*. 8(225).
- Morabito, Carmela. (2013). The Cortical Localization of Language and the “Birth” of the Cognitive Neurosciences. *Rivista Internazionale di Filosofia e Psicologia*. 4.
- Mount, C. W., & Monje, M. (2017). Wrapped to Adapt: Experience-Dependent Myelination. *Neuron*, 95(4), 743–756.
- Mouton, P. R., Gokhale, A. M., Ward, N. L., and West, M. J. (2002). Stereological length estimation using spherical probes. *J. Microsc*. 206, 54–64.
- Möller HE, Bossoni L, Connor JR, Crichton RR, Does MD, Ward RJ, Zecca L, Zucca FA, Ronen I. (2019). Iron, Myelin, and the Brain: Neuroimaging Meets Neurobiology. *Trends Neurosci*. 42(6), 384-401.
- Nieuwenhuys R. (2013). The myeloarchitectonic studies on the human cerebral cortex of the Vogt-Vogt school, and their significance for the interpretation of functional neuroimaging data. *Brain Struct Funct*. 218(2), 303-52.
- Nikolajsen, G. N., Kotynski, K. A., Jensen, M. S., and West, M. J. (2015). Quantitative analysis of the capillary network of aged APP^{swe}/PS1^{dE9} transgenic mice. *Neurobiol. Aging*, 36, 2954–2962.
- Ouda L, Druga R, Syka J. (2012). Distribution of SMI-32-immunoreactive neurons in the central auditory system of the rat. *Brain Struct Funct*. 217(1), 19-36.
- Penfield, W., & Jasper, H. (1954). *Epilepsy and the functional anatomy of the human brain*. Little, Brown & Co.

- Pistorio A. L., Hendry S. H. and Wang X.(2006). A modified technique for high-resolution staining of myelin. *J Neurosci Methods* 153(1), 135-146.
- Purger D, Gibson EM, Monje M. (2016). Myelin plasticity in the central nervous system. *Neuropharmacology*. 110(Pt B), 563-573.
- Rauschecker, JP, Tian, B. (2000). Mechanisms and streams for processing of "what" and "where" in auditory cortex. *Proc Natl Acad Sci U S A*, 97, 11800-11806.
- Reale RA, Imig TJ. (1980). Tonotopic organization in auditory cortex of the cat. *The Journal of Comparative Neurology*, 192, 265-291.
- Ryugo DK, Menotti-Raymond M. (2012). Feline deafness. *Vet Clin North Am Small Anim Pract*. 42(6), 1179-207.
- S. Polyak. The vertebrate visual system, The University of Chicago Press, Chicago (1957)
- Sanides, F. (1969). Comparative architectonics of the neocortex of mammals and their evolutionary interpretation. *Ann. N. Y. Acad. Sci.* 167, 404–423.
- Savoy RL. (2001). History and future directions of human brain mapping and functional neuroimaging. *Acta Psychol (Amst)*, 107(1-3), 9-42.
- Scantlebury, N., Cunningham, T., Dockstader, C., Laughlin, S., Gaetz, W., Rockel, C., Mabbott, D. (2014). Relations between White Matter Maturation and Reaction Time in Childhood. *Journal of the International Neuropsychological Society*, 20(1), 99-112.
- Schmierer K, Scaravilli F, Altmann DR, Barker GJ, Miller DH. (2004). Magnetization transfer ratio and myelin in postmortem multiple sclerosis brain. *Ann Neurol*, 56(3), 407-15.
- Scholz, J., Klein, M. C., Behrens, T. E., & Johansen-Berg, H. (2009). Training induces changes in white-matter architecture. *Nature neuroscience*, 12(11), 1370–1371.
- C.E. Schreiner, J.V. Urbas. (1988). Representation of amplitude modulation in the auditory cortex of the cat. II. Comparison between cortical fields. *Hear. Res.*, 32, 49-64.
- Sherman, D., Brophy, P. (2005). Mechanisms of axon ensheathment and myelin growth. *Nat Rev Neurosci*, 6, 683–690.
- Shors TJ, Matzel LD. (1997). Long-term potentiation: what's learning got to do with it? *Behav Brain Sci.*, 20(4), 597-614; discussion 614-55.
- Simpson D. (2005). Phrenology and the neurosciences: contributions of F. J. Gall and J. G. Spurzheim. *ANZ J Surg.*, 75(6), 475-82.

- Stadelmann C, Timmler S, Barrantes-Freer A, Simons M. (2019). Myelin in the Central Nervous System: Structure, Function, and Pathology. *Physiol Rev.*, 99(3), 1381-1431.
- Stewart DL, Starr A. (1970). Absence of visually influenced cells in auditory cortex of normal and congenitally deaf cats. *Exp Neurol*, 28, 525-528.
- Tyler KL, Malessa R. (2000). The Goltz-Ferrier debates and the triumph of cerebral localizationalist theory. *Neurology*, 55(7), 1015-24.
- Vogt C, Vogt O (1911) Nouvelle contribution à l'étude de la myéloarchitecture de l'écorce cérébrale. *Congres des médecins aliénistes et neurologistes de France, Brüssel*
- Weiskopf N, Mohammadi S, Lutti A, Callaghan MF. (2015). Advances in MRI-based computational neuroanatomy: from morphometry to in-vivo histology. *Curr Opin Neurol.*, 28(4), 313-22.
- West M. J. (2018). Space Balls Revisited: Stereological Estimates of Length With Virtual Isotropic Surface Probes. *Frontiers in neuroanatomy*, 12, 49.
- Williamson JM, Lyons DA. (2018). Myelin Dynamics Throughout Life: An Ever-Changing Landscape? *Front Cell Neurosci.*, 12, 424.
- Zilidou VI, Frantzidis CA, Romanopoulou ED, Paraskevopoulos E, Douka S and Bamidis PD (2018) Functional Re-organization of Cortical Networks of Senior Citizens After a 24-Week Traditional Dance Program. *Front. Aging Neurosci.*, 10, 422.

Appendix A

Table 1: Coefficient of Error Values for Each ROI Across Both Cats

Subregion	Cat 1			Cat 2		
	Infra.	Gran.	Supra.	Infra.	Gran.	Supra.
A1	0.04	0.05	0.04	0.04	0.05	0.04
A2	0.05	0.05	0.05	0.07	0.06	0.06
AAF	0.05	0.06	0.07	0.06	0.06	0.06
FAES	0.05	0.07	0.05	0.06	0.06	0.05
DZ	0.05	0.06	0.05	0.04	0.06	0.05
IN	0.04	0.05	0.06	0.05	0.06	0.06
T	0.04	0.05	0.06	0.06	0.08	0.1
VAF	0.09	0.08	0.08	0.08	0.08	0.08
PAF	0.04	0.05	0.05	0.05	0.06	0.05
VPAF	0.05	0.07	0.09	0.06	0.07	0.07
vPE	0.04	0.06	0.07	0.05	0.06	0.07
dPE	0.06	0.06	0.07	0.04	0.05	0.06
iPE	0.05	0.06	0.06	0.04	0.06	0.06

Curriculum Vitae

Name: Austin Robertson
Post-secondary Education and Degrees: University of Guelph
Guelph, Ontario, CA
2016-2020 BSc Biomedical Sciences

The University of Western Ontario
London, Ontario, Canada
2020-Present MSc Neuroscience

Honours and Awards: Neuroscience Travel Award
2022

Related Work Experience Teaching Assistant
The University of Western Ontario
2020-2022

Poster Presentations:

Robertson, A., Miller, DJ., Butler, B. (2022). Myeloarchitectonic Maps of Cat Auditory Cortex. Presented at Canadian Association for Neuroscience meeting, May 2022.

Talks given:

Robertson, A., Miller, DJ., Butler, B. (2022). Myeloarchitectonic Maps of Cat Auditory Cortex. Presented at Western Neuroscience Research Day, Feb 2022.